https://doi.org/10.5194/bg-2022-181
Preprint. Discussion started: 15 September 2022

Biogeosciences Discussions
Open Access
EGU

The dispersal of fluvially discharged and marine, shelf-produced particulate organic matter in the northern Gulf of Mexico

Yord W. Yedema[1], Francesca Sangiorgi[1], Appy Sluijs[1], Jaap S. Sinninghe Damsté[1,2], Francien Peterse[1]

[1] Department of Earth Sciences, Utrecht University, 3584 CB Utrecht, the Netherlands
[2]Department of Marine Microbiology and Biogeochemistry, NIOZ Royal Netherlands Institute for Sea Research, Den Burg, the Netherlands

Correspondence to: Yord W. Yedema (y.w.ijedema@uu.nl)

https://doi.org/10.5194/bg-2022-181
Preprint. Discussion started: 15 September 2022

Biogeosciences Discussions Open Access EGU

Abstract. Rivers play a key role in the global carbon cycle by transporting terrestrial organic matter (TerrOM) from land to the ocean. Upon burial in marine sediments, this TerrOM may be a significant long-term carbon sink, depending on its composition and properties. However, much remains unknown about the dispersal of different types of TerrOM in the marine realm upon fluvial discharge as the commonly used bulk OM parameters do not reach the required level of source- and process-specific information. Here, we analysed bulk OM properties, lipid biomarkers (long-chain *n*-alkanes, sterols, long-chain diols, alkenones, branched and isoprenoid glycerol dialkyl glycerol tetraethers (GDGTs)), pollen, and dinoflagellate cysts in marine surface sediments along two transects offshore the Mississippi and Atchafalaya Rivers (MAR), as well as one along the 20 m isobath in the direction of the river plume. We use these biomarkers and palynological proxies to identify the dispersal patterns of soil-, fluvial, higher plant, and marine produced OM in the coastal sediments of the northern Gulf of Mexico (GoM).

The Branched and Isoprenoid Tetraether (BIT) index and the relative abundance of C_{32} 1,15-diols indicative for freshwater production show high contributions of soil and fluvial OC near the Mississippi River mouth (BIT = 0.6, $F_{C32\ 1,15}$ >50%), which rapidly decrease further away from the river mouth (BIT <0.1, $F_{C32\ 1,15}$ <20%). In contrast, concentrations of long-chain *n*-alkanes and pollen grains do not show this stark decrease along the path of transport, and especially *n*-alkanes are also found in sediments in deeper waters. Proxy indicators show that marine productivity is highest close to shore, and reveal that marine producers (diatoms, dinoflagellates, coccolithophorids) have different spatial distributions, indicating their preferential niches. Close to the coast, where food supply is high and waters are turbid, cysts of heterotrophic dinoflagellates dominate the assemblages. The dominance of heterotrophic taxa in shelf waters in combination with the rapid decrease in the relative contribution of TerrOM towards the deeper ocean, suggests that TerrOM input may trigger a priming effect that results in its rapid decomposition upon discharge. In the open ocean far away from the river plume, autotrophic/phototrophic dinoflagellates dominate the assemblages, indicating more oligotrophic conditions.

Our multi-disciplinary approach reveals that different types of TerrOM have distinct dispersal patterns, suggesting that the initial composition of this particulate OM influences the burial efficiency of TerrOM on the continental shelf and open ocean.

1 Introduction

The transport of terrestrial organic matter (TerrOM) from land to the sea, and subsequent discharge into the (open) ocean is an important process that connects the terrestrial and marine carbon cycles (Blair & Aller, 2012). This process is mostly conducted by rivers. Most TerrOM that enters the river originates from soil mobilisation and weathering of rocks and includes plant-derived, soil-derived, and petrogenic OM, as well as aquatic OM produced in lakes and streams. In rivers, TerrOM can be transported as particulate organic carbon (POM) or dissolved organic carbon (DOM), where POM often includes old, degraded plant and soil material, while DOM is generally younger (Mayorga et al., 2005). During river transport, partial degradation and/or (temporal) storage in sediments and inland wetlands can change the composition of

https://doi.org/10.5194/bg-2022-181
Preprint. Discussion started: 15 September 2022

TerrOM (Battin et al., 2009; Aufdenkampe et al., 2011). Therefore, only a fraction of the OM delivered to rivers (32-47%) reaches the coastal zone (Cole et al., 2007; Battin et al., 2009; Tranvik et al., 2009; Aufdenkampe et al., 2011; Regnier et al., 2013; Li et al., 2017; Kirschbaum et al., 2019).

After its arrival in the ocean, TerrOM may be buried in marine sediments, where it can form a long-term sink of atmospheric CO_2 (Hedges et al., 1997), but burial rates in coastal zones are not homogeneous. Regions that receive substantial input of OM, such as river-dominated continental shelves, form potential hotspots for OM burial (e.g., Bianchi et al., 2018). On a global scale, it is estimated that only ~one-third of the fluvially discharged POM is eventually preserved in marine sediments (Burdige, 2005; Blair and Aller, 2012), indicating that part of the TerrOM is lost in the marine realm. The dispersal of TerrOM in the marine realm depends on many factors, including its molecular composition, the mode of transport, the recalcitrance/ degradability of TerrOM and oxygen exposure time (e.g., Zonneveld et al., 2010). One component that is often overlooked in marine sediments is the relative contribution of different sources of TerrOM (i.e., microbial, plant, aquatic) that make up its composition. Since the contribution of TerrOM to marine sediments is often investigated using bulk parameters only, the composition of TerrOM is not generally characterized, whereas the different components may have a distinct dispersal patterns and burial efficiencies. In addition, TerrOM contributions to marine sediments might be masked if only bulk parameters are used, thereby influencing our understanding of TerrOM dispersal patterns in the marine environment (e.g., Goñi et al., 1997).

The northern Gulf of Mexico (GoM) is a region that receives high inputs of OM from the Mississippi-Atchafalaya River (MAR) system. As the MAR catchment area covers a large part of North America, it transports a large variety of TerrOM types from the continent to the ocean, making it an interesting region to investigate the spatial distribution of different TerrOM pools. Here we here aim to disentangle the origin of TerrOM in 20 marine surface sediments offshore the Mississippi and Atchafalaya River delta (Fig. 1) using lipid biomarkers and palynological methods (dinoflagellate cysts, pollen) that are specific for soil-, fluvial-, plant- and marine OM, supported by bulk parameters (total organic carbon (TOC), the organic carbon/total nitrogen ratio (C/N ratio) and bulk $\delta^{13}C_{org}$) of the sediments. In addition, the marine biomarkers are used to identify the preferred niches of different OM producers in the GoM and assess their possible relation to the TerrOM distribution.

https://doi.org/10.5194/bg-2022-181
Preprint. Discussion started: 15 September 2022

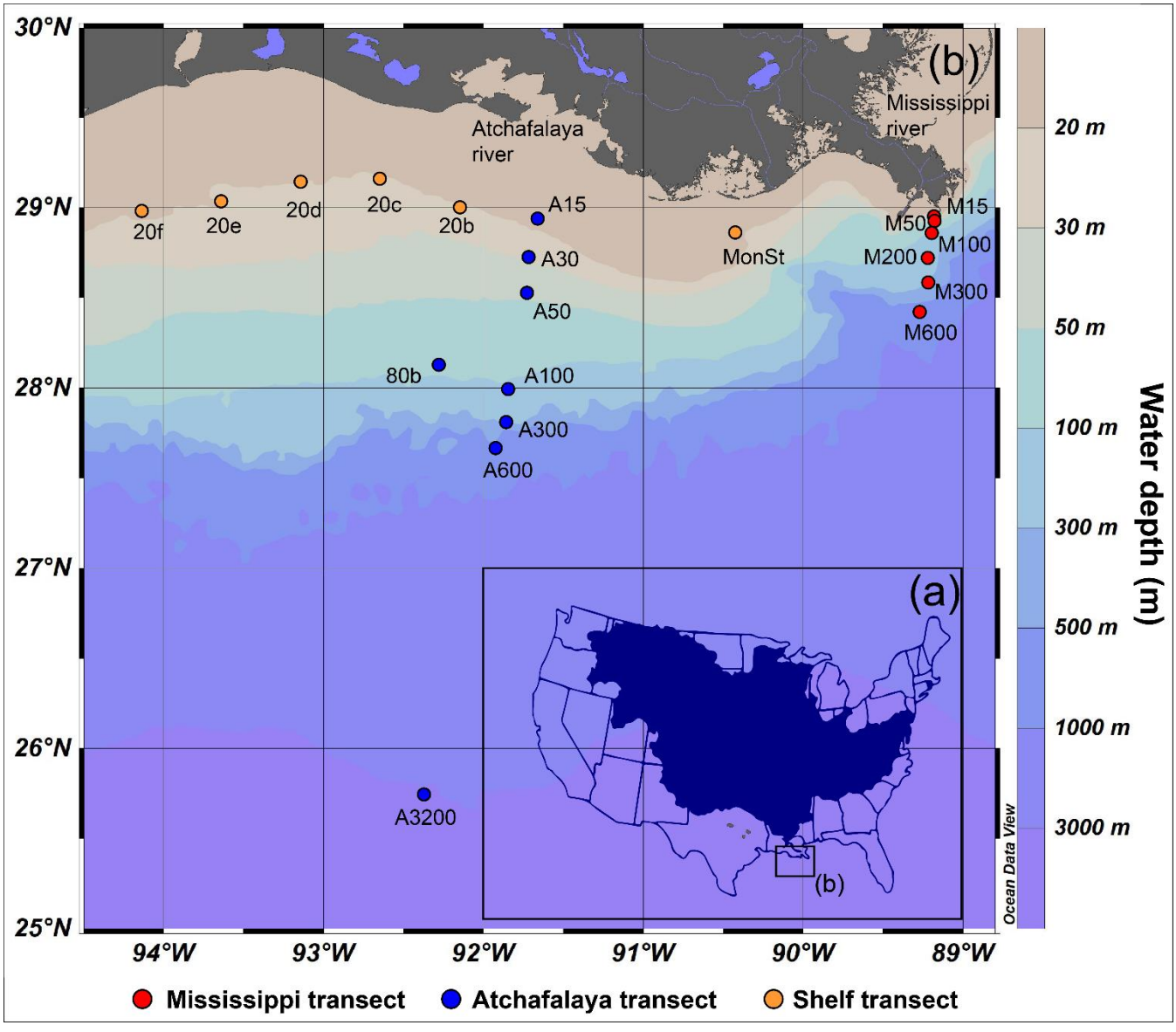

Figure 1: a) The catchment of the Mississippi and Atchafalaya River System, and b) the locations of marine surface sediments in the northern GoM used for this study. Surface sediments have been collected along three transects; the land-sea transects of the Mississippi River (15-600 m water depth, samples M15, M50, M100, M200, M300 and M600) and the Atchafalaya River (15-3200 m water depth, samples A15, A30, A50, 80b, A100, A300, A600 and A3200) and a shelf transect following the river plume at the 20 m isobar (samples 20f, 20e, 20d, 20c, 20b, MonSt). Sample names correspond to Yedema et al., (2022) https://doi.pangaea.de/10.1594/PANGAEA.944838.

https://doi.org/10.5194/bg-2022-181
Preprint. Discussion started: 15 September 2022


Biogeosciences Discussions

2 Proxy background

2.1 Lipid biomarker proxies

To disentangle the composition of OM in the surface sediments of the northern GoM, we use concentrations and ratios of several lipid biomarkers. Glycerol dialkyl glycerol tetraethers (GDGTs) are membrane lipids of marine archaea and a group of largely unknown bacteria, which produce isoprenoid GDGTs (isoGDGTs; Koga et al., 1993), and branched GDGTs (brGDGTs; Sinninghe Damsté et al., 2000), respectively. Although the exact producer(s) of brGDGTs is still unknown, they were initially thought to be solely produced in soils and peats. Based on similarities in their concentration to that of Acidobacteria in a peat profile (Weijers et al., 2009), and the detection of a specific brGDGT in an Acidobacterial culture (Sinninghe Damsté et al., 2011, 2018), the phylum of Acidobacteria likely hosts their source organisms, although other bacterial phyla cannot be discarded (Weber et al., 2018; De Jonge et al., 2021). The Branched and Isoprenoid Tetraether (BIT) index (Hopmans et al., 2004), uses the presumed soil origin of brGDGTs relative to that of crenarchaeol, an isoGDGT that is exclusively produced by Thaumarchaeota (Sinninghe Damsté et al., 2002), to determine the relative input of soil-derived OM in a marine environment. Accordingly, high BIT index indicates more soil input and a low BIT index a larger marine contribution to the sediment. However, recent studies have shown that brGDGTs can also be produced in rivers (e.g., Zell et al., 2013; De Jonge et al., 2014a), lakes (e.g., Weber et al., 2018; van Bree et al., 2020) and the coastal marine environment (e.g., Peterse et al., 2009; Zhu et al., 2011; Sinninghe Damsté, 2016), while also crenarchaeol can be produced in soils (Weijers et al., 2006), and thus the BIT index should be applied with care in the assessment of terrestrial OM sources. Fluvial and marine in situ contributions to the brGDGT pool can be recognized by distinct traits in their molecular structure. For example, brGDGTs produced in rivers appear to be dominated by compounds that have a methylation at the C-6 position of their alkyl chain(s), as opposed to position C-5 that is more common for brGDGTs occurring in soil (De Jonge et al., 2014b; Warden et al., 2016; Kirkels et al., 2020). This difference can be quantified using the Isomer Ratio (IR), where a higher IR indicates a larger contribution of 6-methyl brGDGTs (De Jonge et al., 2014b). In addition, brGDGTs produced in the coastal marine environment can be recognised by a higher number of cyclopentane rings present in the tetramethylated brGDGTs, which is captured in the $\#rings_{tetra}$ ratio (Sinninghe Damsté, 2016). A value of >0.7 of the $\#rings_{tetra}$ ratio is considered to represent a non-soil contribution to the signal, as these values are typically not reached in modern surface soils, but are common in alkaline shelf sediments of the ocean (Sinninghe Damsté, 2016).

We use the concentration of the isoGDGT crenarchaeol in the GoM sediments to constrain the ecological niche of Thaumarchaeota, which are ammonia oxidizers and, therefore, play an important role in the nitrogen cycle (e.g., Wuchter et al., 2006). As ammonia is an important breakdown product produced during the degradation of marine OM, the concentration of crenarchaeol can be used as a proxy for marine productivity.

Long-chain diols are biomarkers characterized by a long *n*-alkyl chain and two alcohol groups, attached at the C-1 and a mid-chain position. In marine settings, the diols that are commonly found are C_{28} and C_{30} 1,13-diols, the C_{28} and C_{30} 1,14-diols and the C_{30} and C_{32} 1,15-diols. The 1,14-diols have been detected in *Proboscia* diatoms (Sinninghe Damsté et al.,

https://doi.org/10.5194/bg-2022-181
Preprint. Discussion started: 15 September 2022

2003). Also the 1,13- and 1,15- C_{28} and C_{30} diols are commonly found in marine settings, although their main source remains unclear (Rampen et al., 2012; Balzano et al., 2018). In contrast, C_{32} 1,15-diols have been found in freshwater lakes and stagnant waters where they are produced by eustigmatophyte algae (Volkman et al., 1992; Shimokawara et al., 2010; Lattaud et al., 2021). Based on high fractional abundances of the C_{32} 1,15-diol in coastal zones receiving significant river input (Rampen et al., 2014a; de Bar et al., 2016), Lattaud et al. (2017) proposed that its relative abundance compared to the C_{28} 1,13- and C_{30} 1,13- and 1,15 diols (expressed in the $F_{C32\ 1,15}$ ratio) could be used as a proxy for fluvial organic matter input in coastal zones. In addition, we will use the concentration of the 1,14-diols as an indicator of diatom productivity.

Long-chain *n*-alkanes are derived from the epicuticular waxes of higher plants and widely used as markers for higher plants (Eglinton and Hamilton, 1963). These leaf waxes can be transported to the marine realm by fluvial and aeolian transport (Gagosian et al., 1987). A strong odd-over-even carbon number predominance is an indication that the *n*-alkanes are derived from higher plants and is quantified in the Carbon Preference Index (CPI; Bray and Evans, 1961). The chain length of *n*-alkanes is presumed to be influenced by climate, where longer chain lengths are linked to warmer and drier conditions (Poynter et al., 1989). The Average Chain Length (ACL) is thus commonly used as indicator of vegetation type, where grasses produce *n*-alkanes with longer chain lengths than trees and shrubs (Bray and Evans, 1961). Here, we use the concentration of odd carbon numbered *n*-alkanes derived from higher plants in a specific range (C_{29}-C_{35}) as a proxy for terrestrial plant input.

Higher plants furthermore produce sterols like campesterol, stigmasterol and β-sitosterol (Volkman, 1986; Meyers, 1997; Lütjohann, 2004), the presence of which has been used as a proxy for plant-derived OM (e.g., Xiao et al., 2013; Rontani et al., 2014). However, algal sources of these sterols have also been identified in marine algae (Rampen et al., 2010; Volkman, 2016). This hampers the use of these sterols as specific markers for higher plants and requires comparison with other plant markers. Similarly, brassicasterol and dinosterol are often associated with diatoms and dinoflagellates, respectively, although other marine algal groups can also produce these sterols (Volkman, 2016; Sangiorgi et al., 2005; Rampen et al., 2010). We here use these sterols as additional proxies for marine OM and possibly higher plant OM, after careful comparison with other terrestrial and marine OM proxies.

Finally, we will use the presence and concentration of *n*-C_{37} alkenones that are produced by haptophyte algae (Volkman et al., 1980) as indicators for marine productivity by haptophytes.

2.2 Palynological proxies

Dinoflagellate cysts, pollen and spores were used as proxies for marine primary productivity and plant input, respectively. Dinoflagellates are protists that live in the upper water column and ~15% of the species produce organic-walled resting cysts (dinocysts) during their life cycle (Head, 1996). Dinocysts can be preserved in sediments and their assemblages can be used as proxies for surface waters nutrient availability and productivity, upwelling, salinity, and temperature (Reid and Harland, 1977; Rochon et al., 1999; Zonneveld et al., 2013). Most dinoflagellate species are obligate autotrophs or heterotrophs, some are mixotrophs. Autotrophic species are commonly found in the photic zone, while heterotrophic species feed on organic

https://doi.org/10.5194/bg-2022-181
Preprint. Discussion started: 15 September 2022

debris and other organisms, including diatoms, bacteria, and other dinoflagellates, and therefore live in water with high primary productivity and/or organic matter input (e.g., Gaines and Taylor, 1984). For this reason, the percentage of cysts of heterotrophic dinoflagellates in assemblages is used to indicate primary productivity (e.g., Sangiorgi and Donders, 2004). It has been argued that the total dinocyst concentration (number dinocysts g^{-1} sediment) in sediments is a better indicator of dinoflagellate productivity and total primary marine productivity (Zonneveld et al., 2009; Hardy et al., 2016) as cysts of heterotrophic and autotrophic dinoflagellates have different preservation potential (e.g., Zonneveld et al., 2010). Here, we use both the percentage of heterotrophic dinocysts (% Heterotrophs) in the assemblages and the total dinocyst concentration as indicator for marine productivity. To facilitate the comparison between dinocyst concentrations and (marine) biomarker concentrations, we normalised the dinocyst concentrations to g TOC (dinocysts g^{-1} TOC). Routinely, dinocysts concentrations are presented as dinocysts g^{-1} dry sediment.

Pollen grains and spores are produced by vegetation and occur widespread in coastal marine sediments. Most pollen are fluvially transported, resulting in high concentrations in coastal sediments in the proximity of river mouths (e.g., Heusser, 1988). Further offshore, pollen is usually less abundant, and wind-blown pollen (mainly *Pinus*) represent a relatively large contribution to the assemblage (Mudie and McCarthy, 1994; Chmura et al., 1999; Donders et al., 2018). To exclude aeolian transport, *Pinus* pollen was not included in the total pollen concentration. This pollen concentration, normalised to g TOC (pollen g^{-1} TOC), is here used as a proxy for terrestrial plant input transported by rivers.

3 Materials and Methods

3.1 Study site

With a catchment of $3.3*10^6$ km^2 (Milliman and Syvitski, 1992), the MAR is one of the largest river basins worldwide, and the largest watershed in North America (Fig. 1a). It is responsible for the input of over 90% of freshwater, nutrients, and suspended material that accumulate in the northern GoM (Deegan et al., 1986; Rabalais et al., 2007). The Mississippi River (MR) has a mean annual water discharge of ~18,400 m^3/s, while the Atchafalaya River (AR) discharges ~4,400 m^3/s (Bianchi and Allison, 2009; data from USGS). In the 1960s, a control structure was completed in the river, which diverted a combined 30% of the stream flow of the Lower MR and Red River into the AR (Reuss, 2004). Upon discharge, the MAR water flow is directed westward along the Louisiana shelf under the influence of local wind stress. Annual wind patterns in the GoM area are predominantly westward, and wind comes directly from land during winter months (Zavala-Hidalgo et al., 2014). Subsequently, the MAR water flow is predominantly directed westward along the Louisiana shelf upon discharge. Further offshore, the surface circulation is mainly controlled by the Loop Current, which in summer brings oligotrophic Caribbean surface waters to the northern GoM (Sturges and Evans, 1983).

Annual particle loads of the MR and AR reach 115 and 57 Pg/year, respectively. These high loads result in sedimentation rates of >10 cm/year close to the mouths of both rivers (Bianchi et al., 2002; Santschi and Rowe, 2008). The shelf areas of the MAR differ in morphology, which influences the sediment dispersal; the high discharge of the MR has led to rapid delta

https://doi.org/10.5194/bg-2022-181
Preprint. Discussion started: 15 September 2022

progradation, resulting in a steep shelf where most of the suspended particles is transported offshore (Corbett et al., 2006), whereas the AR discharges mainly into the Atchafalaya Bay (Neill and Allison, 2005; Xu et al., 2011), which has resulted in a more gently sloped part of the Louisiana shelf. The MR mouth is located close to the Mississippi canyon, which formation is generally linked to channel entrenchment of the MR during sea level low stands (Coleman et al., 1982).

Highest freshwater discharge generally occurs in early spring, while the peak in nutrient load delivered to the northern GoM happens around June (Rabalais et al., 2007). The combined effect of algal blooms triggered by the high nutrient input and water column stratification in summer months causes the formation of a seasonal hypoxic zone (O_2 concentrations of <2 mg l^{-1}) that currently covers 23,000 km^2 at the seafloor (Rabalais and Turner, 2019). These lower oxygen conditions are most common between 10 and 30 m water depth on the shallow continental shelf in the northern GoM. In the last decades, hypoxic conditions became more widespread due to excess nutrient input from the MR derived from agricultural activities (e.g. Rabalais et al., 2002). While hypoxic events do occur in other months of the year, waters are more oxygenated (>6 mg l^{-1}) in non-summer months (Rabalais and Turner, 2019).

3.2 Sample collection

Marine surface sediments (0-2 cm) were collected during a research cruise with the R/V *Pelagia* in February 2020. Multicores were acquired with an Oktopus multicoring apparatus at 20 locations, covering a transect along the 20 m isobar on the shelf in the direction of the river plume and land-sea transects from the MR and AR at depths ranging from 15-600 m and 15-3200 m, respectively (Fig. 1b). At most sites, the sediment contained of muddy material, except for the western shelf, where the sediments had a more sandy nature. Sediments were stored at -20 °C on board and remained frozen during transport to the laboratory. All sediments were freeze-dried prior to further analysis.

Part of our dataset is located in a seasonal hypoxic zone, that experiences lower oxygen levels in bottom waters in summer (Rabalais et al., 2002). The availability of oxygen represents a large factor in the preservation potential of TerrOM (Hedges et al., 1999) and can therefore influence the dispersal patterns of TerrOM. Regardless, as waters are well oxygenated during the rest of the year, oxygen levels are unlikely to introduce large variations in preservation in the GoM surface sediments.

3.3 Bulk sediment analysis

Freeze-dried and homogenized sediments (ca. 0.3 g) were treated with 1 mL HCl overnight to remove inorganic carbon. The TOC, TN and $\delta^{13}C_{org}$ were analysed using an Elemental Analyzer (Fisons Instruments NA 1500) coupled to an isotope ratio mass spectrometer (IRMS, FinniganMat Delta Plus). TOC and TN are expressed as weight percentage (wt.%) of the dried sediment and have an error of ± 0.01 wt.% (TOC) and ± 0.001 wt.% (TN) based on replicate runs of lab standards. These values were used to derive the molar C/N ratios. The $\delta^{13}C_{org}$ values are reported relative to the Vienna Pee Dee Belemnite standard (VPDB). Reproducibility of $\delta^{13}C_{org}$ measurements was usually better than 0.04‰ based on lab standards.

https://doi.org/10.5194/bg-2022-181
Preprint. Discussion started: 15 September 2022

3.4 Lipid biomarker analysis

Lipid biomarkers were extracted from ~1 g of freeze dried and homogenized sediment with 25 mL of dichloromethane (DCM):methanol (9:1, v/v), using the microwave extraction system Milestone Ethos X (MEX). The total lipid extract was passed over a small sodium sulphate column to remove any remaining water prior to separation into an apolar, neutral and polar fraction, by passing it over a small column with activated aluminium oxide and solvent mixtures of hexane:DCM (9:1), hexane:DCM (1:1) and DCM:methanol (1:1) as the respective eluents.

The apolar and neutral fractions, containing *n*-alkanes and alkenones, respectively, were dissolved in 10 µL hexane and co-injected with an external squalene standard on-column on a gas chromatograph coupled to a flame ionisation detector (GC-FID, Hewlett Packard 6890 series). The GC-FID was operated with helium as carrier gas at a constant pressure of 100 kPa, and an oven temperature starting at 70 °C and rising first to 130 °C at 20 °C min^{-1} and then to 320 °C at 4 °C min^{-1}, at which it was held for 10 min. Concentrations of *n*-alkanes and alkenones were determined by relating their peak areas with that of the squalene standard. The CPI and ACL were calculated using the equations from Marzi et al. (1993) and Poynter et al. (1989), respectively:

$$CPI = ((C_{23} + C_{25} + C_{27} + C_{29} + C_{31} + C_{33}) + (C_{25} + C_{27} + C_{29} + C_{31} + C_{33} + C_{35})) / (2 * (C_{24} + C_{26} + C_{28} + C_{30} + C_{32} + C_{34})) \quad (1)$$

$$ACL = (25C_{25} + 27C_{27} + 29C_{29} + 31C_{31} + 33C_{33} + 35C_{35})/(C_{25} + C_{27} + C_{29} + C_{31} + C_{33} + C_{35}) \quad (2)$$

A known amount of a synthetic C_{46} glycerol trialkyl glycerol tetraether (GTGT) standard was added to the polar fraction, which was subsequently dissolved in 1.5 mL hexane:isopropanol (99:1, v/v) and passed over a 45 µm polytetrafluorethylene (PTFE) filter. Analysis of GDGTs was done using high performance liquid chromatography/mass spectrometry (HPLC/MS) using the method of Hopmans et al. (2016). Peaks were detected via selected ion monitoring (SIM), using m/z 744 for the internal standard, m/z 1302, 1300, 1298, 1296 and 1292 for isoGDGTs and m/z 1050, 1036, 1034, 1032, 1022, 1020 and 1018 for brGDGTs. For GDGT proxy calculations, the roman numerals refer to the concentrations of the GDGTs as listed in Sinninghe Damsté, (2016). The BIT index was calculated according to Hopmans et al. (2004) and includes the 5- and 6-methyl brGDGTs:

$$BIT = [(Ia) + (IIa) + (IIIa) + (IIa') + (IIIa')]/[(Ia) + (IIa) + (IIIa) + (IIa') + (IIIa') + (Cren)] \quad (3)$$

The isomer ratio (IR) expresses the fractional abundance of 6-methyl brGDGTs over 5- and 6-methyl brGDGTs (De Jonge et al., 2014b):

$$IR = [(IIa') + (IIb') + (IIc') + (IIIa') + (IIIb') + (IIIc')]/[(IIa') + (IIb') + (IIc') + (IIIa') + (IIIb') + (IIIc') + (IIa) + (IIb) + (IIc) + (IIIa) + (IIIb) + (IIIc)] \quad (4)$$

The number of rings of tetramethylated brGDGTs ($\#rings_{tetra}$) was calculated using the equation of Sinninghe Damsté (2016):

$$\#rings_{tetra} = [(Ib) + 2*(Ic)/[(Ia) + (Ib) + (Ic)] \quad (5)$$

https://doi.org/10.5194/bg-2022-181
Preprint. Discussion started: 15 September 2022

Diols and sterols were analysed by silylation of an aliquot of the polar fraction, using 10 µL pyridine and 10 µL N_2O-bis(trimethylsilyl)trifluoroacetamide (BSTFA) and heating to 60 °C for 20 min. The silylated fractions were dissolved in 30 µL ethyl acetate and co-injected with the squalene standard on-column on the GC-FID. For peak identification and qualitative integration, each sample was also analysed using GC- mass spectrometry (Thermo Trace Ultra GC connected to Finnigan Trace DSQ mass spectrometry, GC-MS DSQ), with a mass range *m/z* 50-800, using helium as carrier gas with a constant flow rate of 2.0 ml/min. Diols that were considered for analysis were C_{28} 1,14 (m/z 299), C_{28} 1,13, C_{30} 1,15 (m/z 313), C_{30} 1,14 (m/z 327), C_{30} 1,13 and C_{32} 1,15 (m/z 341). The $F_{C32\ 1,15}$ is calculated according to Lattaud et al. (2017) and uses the areas of the 1,13-and 1,15-diols:

$$F_{C32\ 1,15} = (AC_{32}\ 1,15 / (AC_{32}\ 1,15 + AC_{30}\ 1,15 + AC_{28}\ 1,13 + AC_{30}\ 1,13)) * 100 \quad (6)$$

Concentrations for all biomarkers have been normalized to TOC.

3.5 Palynological processing

Freeze dried and homogenized sediments (ca. 20 g) were selected for palynological analysis. A *Lycopodium clavatum* tablet containing 19,855 spores (± 2.62%) was added to each sample to enable dinocysts, and pollen and spores quantification (Stockmarr, 1971; Wood, 1996). Sediments were treated with 30% HCl and 40% cold HF at room temperature to remove carbonates and silicates, respectively. No oxidation was performed. After acid treatment, the sediments were sieved using a fine mesh and an ultrasonic bath to isolate the 10-250 µm fraction. Subsequently, residues were made and mounted on microscope slides with glycerine jelly. Between 116 and 245 dinocysts (median 203) and 186 – 300 pollen grains (median 258) were counted using optical microscopy at 400x magnification. The dinocyst taxonomy follows Williams et al. (2017) and dinocysts were identified following Rochon et al. (1999) and Zonneveld and Pospelova (2015). Pollen and spores identification was based on Willard et al. (2004).

3.7 Data processing

Isosurface plots were constructed using Ocean Data View software (Schlitzer, 2015), using weighted average gridding. Principle Component Analysis (PCA) was performed on relative concentrations of biomarkers, pollen, and dinoflagellate cysts using Past version 4.04 (Hammer et al., 2001), where all biomarker, pollen and dinoflagellate cyst concentrations were normalized against their maximum value (min-max normalization) to facilitate comparison between all proxies.

4 Results

4.1 Bulk parameters

The total organic carbon (TOC) content (in wt%) of the surface sediments varied between 0.05 and 1.63 wt% and was much lower (≤0.65%) on the western portion of the shelf than close to the MAR (>1.42%) or offshore (Fig. 2a). The molar C/N

https://doi.org/10.5194/bg-2022-181
Preprint. Discussion started: 15 September 2022

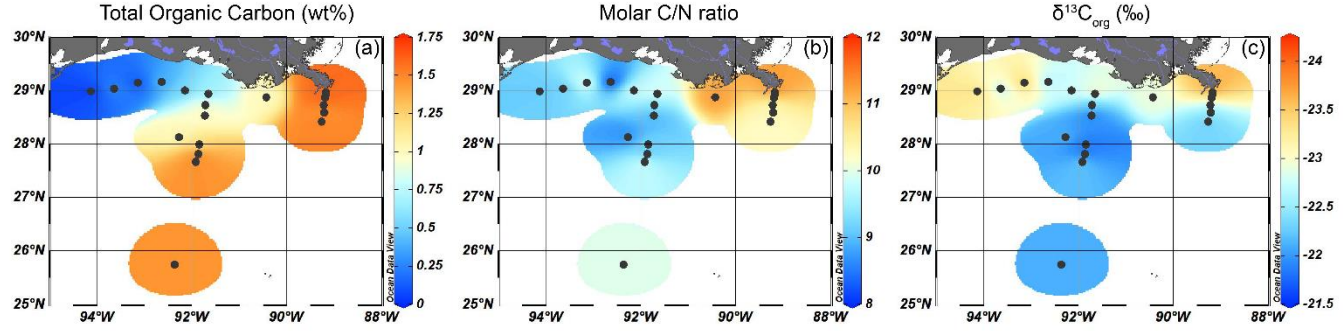

Figure 2: Isosurface plots for bulk sediment properties for surface sediments in the GoM for a) TOC content (wt%), b) the molar C/N ratio, c) $\delta^{13}C_{org}$ (‰).

4.2 Lipid biomarkers

BrGDGTs were detected at all sites, with concentrations of 40-70 µg g^{-1} TOC close to the MR, decreasing to <20 µg g^{-1} TOC on the shelf, and then to <10 µg g^{-1} TOC in the deeper ocean (Fig. 3a). Crenarchaeol was the most dominant isoGDGT (mean 65 ± 5% of all isoGDGTs) with absolute concentrations varying between 30 and 400 µg g^{-1} TOC. Concentrations of crenarchaeol were lowest close to the MR, and then increased towards the shelf. In the surface sediments in deeper waters (> 100 m), crenarchaeol concentrations were always >90 µg g^{-1} TOC (Fig. 4a). These concentrations translate into BIT index values ranging from 0.14-0.57 close to the MR with lower values (<0.10) towards open sea (Fig. 3b).

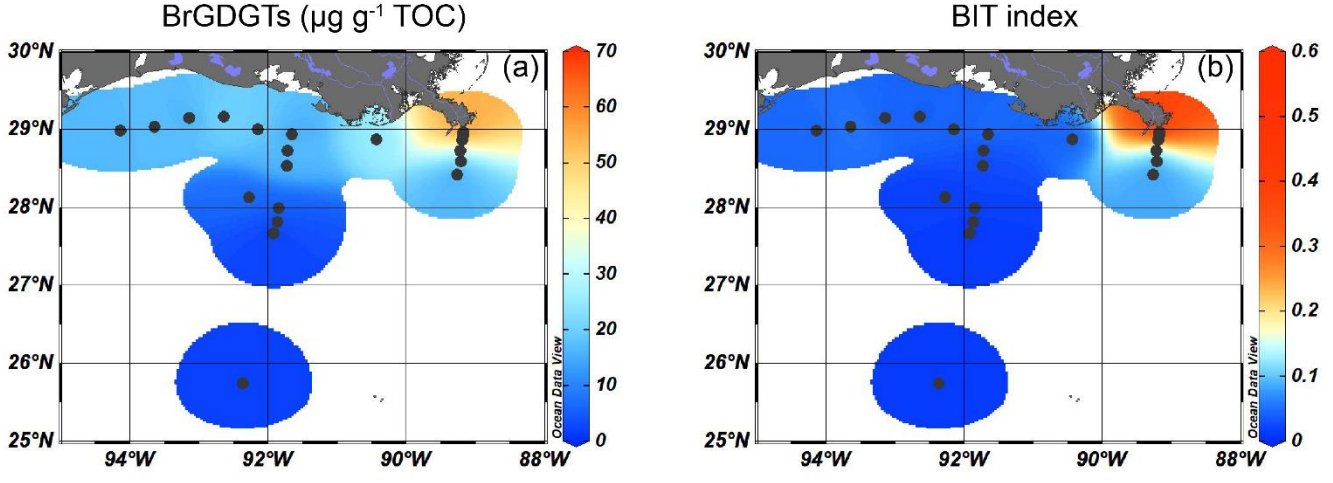

https://doi.org/10.5194/bg-2022-181
Preprint. Discussion started: 15 September 2022

Figure 3: Isosurface plots for proxies for soil-derived TerrOC input for surface sediments in the GoM: a) the concentration of brGDGTs (μg g^{-1} TOC), and b) the BIT index.

Long-chain diols were detected at 19 of the 20 sites, with concentrations ranging from 7 – 70 μg g^{-1} TOC. At the westernmost shelf location, where the TOC concentration was the lowest (0.05 wt%), diols were not detected. The highest concentration of 1,14-diols was found on the shelf and on the shallow part (<100 m water depth) of the Atchafalaya transect (12-18 μg g^{-1} TOC), with lower concentrations on the Mississippi transect and in deeper waters (<8 μg g^{-1} TOC, Fig. 4b). The absolute abundance of the C_{32} 1,15-diol varied from 1 μg g^{-1} TOC in the deepest waters to >10 μg g^{-1} TOC on the shelf close to the AR (Fig. 5a), while the $F_{C32\ 1,15}$ ranged from 6-51% and showed a trend with higher values close to the MR mouth, and lower values further away (Fig. 5b).

https://doi.org/10.5194/bg-2022-181
Preprint. Discussion started: 15 September 2022

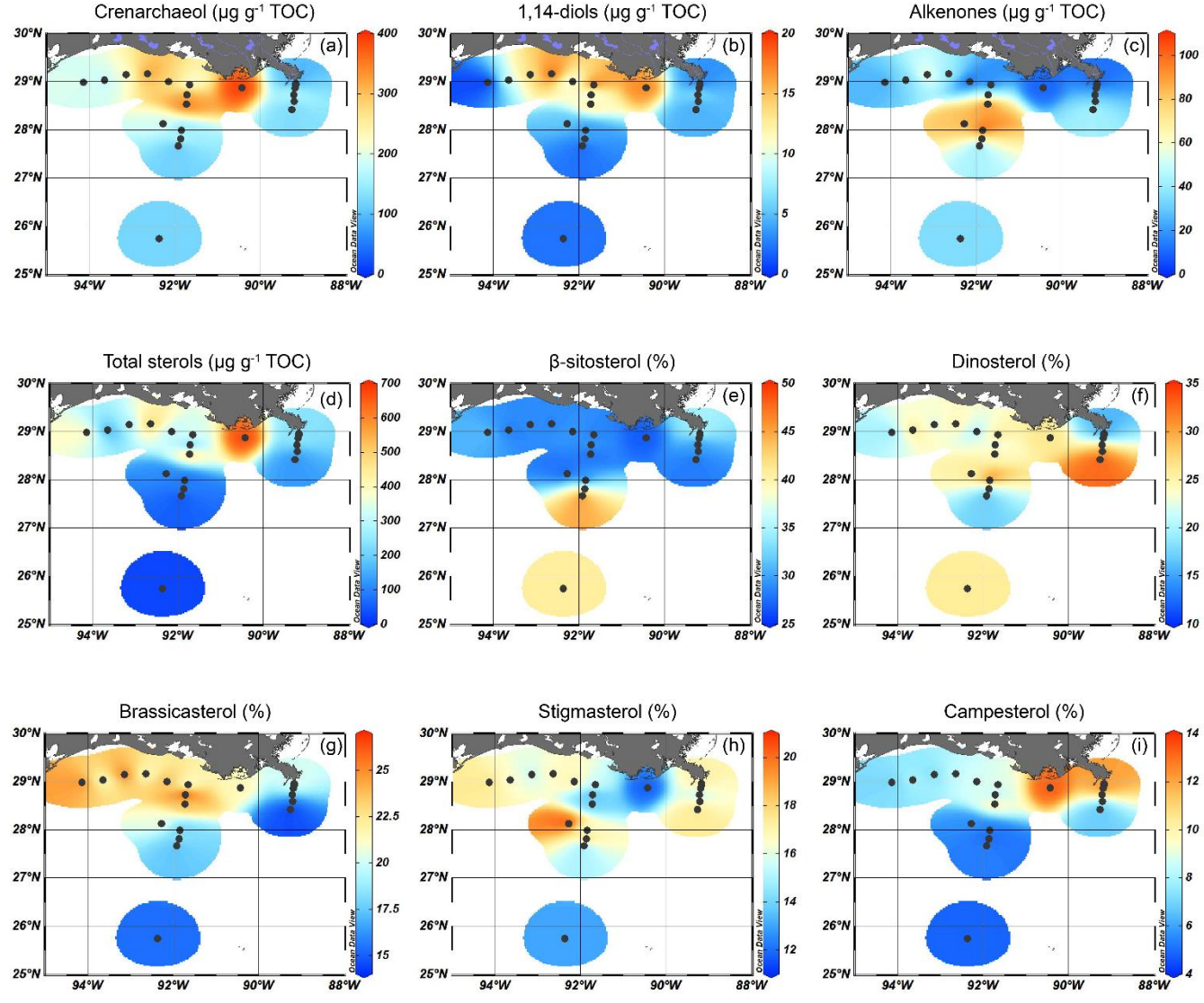

Figure 4: Marine OC production in the GoM, as indicated by isosurface plots of TOC-normalized concentrations of a) crenarchaeol produced by Thaumarchaeota, b) long-chain 1,14-diols produced by *Proboscia* diatoms, c) alkenones produced by haptophyte algae, and d) sterols (β-sitosterol, dinosterol, brassicasterol, stigmasterol and campesterol). Isosurface plots e-i show the relative abundances of these sterols.

https://doi.org/10.5194/bg-2022-181
Preprint. Discussion started: 15 September 2022

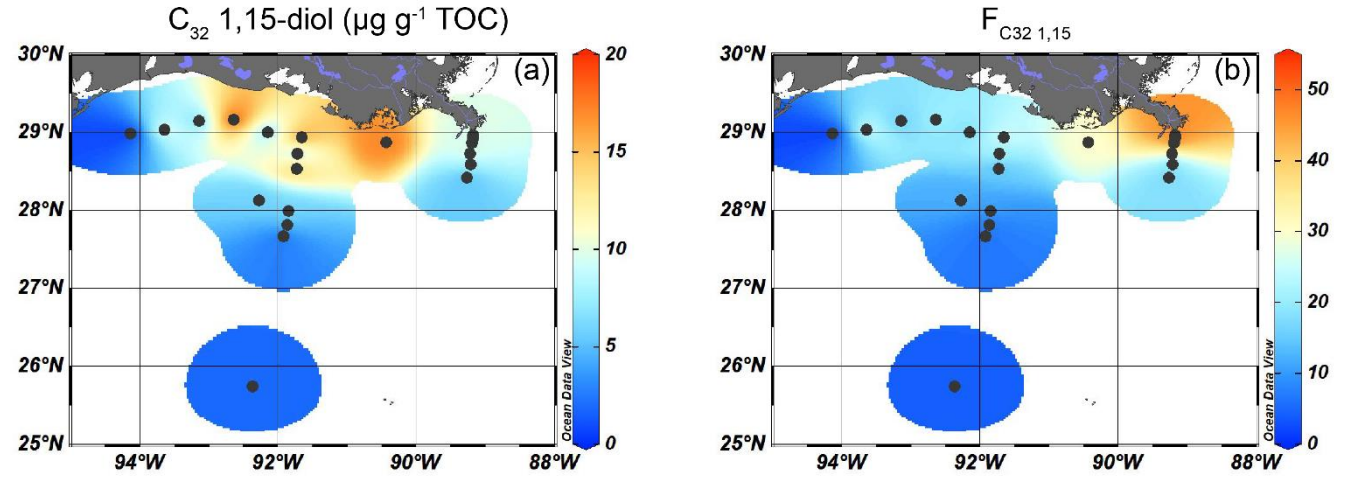

Figure 5: Isosurface plots of proxies for fluvially-derived TerrOC input for surface sediments in the GoM: a) the concentration of C_{32} 1,15-diols (µg g^{-1} TOC) and b) the $F_{C32\ 1,15}$ index.

Alkenones were mostly found in sediments from a water depth between 50 and 300 m in the Atchafalaya transect (70 – 110 µg g^{-1} TOC), while their abundance in sediments from the shelf and from deeper waters was much lower (3 – 60 µg/ g^{-1} TOC) (Fig. 4c).

Five sterols were identified at all sites. Total sterol concentrations ranged from 25 µg g^{-1} TOC in deeper waters, to >400 µg g^{-1} TOC on the shelf (Fig. 4d). The highest sterol concentrations (677 µg g^{-1} TOC) were found in between the MR and AR deltas. Due to the presumed mixed sources of these individual sterols, their relative abundance was also plotted to identify spatial differences in their occurrence (Fig. 4e-i). β-sitosterol was the most abundant, accounting for ~30% of the sterol assemblage on the shelf and up to 48% in deeper waters, where total sterol concentrations were low (Fig. 4e). Dinosterol was most abundant at the deeper MR and AR transects (>25% of total sterols), while brassicasterol was most abundant on the shelf and close to the MR (>20%) (Fig. 4f, g). The relative abundance of stigmasterol was highest in sediments from ca. 80 m water depth of the Atchafalaya transect (20%), while that of campesterol was high close to the MR (13%), Fig. 4h,i).

Long-chain *n*-alkane (C_{29}-C_{35}) concentrations varied between 23 and 210 µg g^{-1} TOC. They were most abundant near the mouth of the MAR but were also consistently present on the shelf and more seaward, albeit in increasingly lower concentrations (from 70-130 to ~50 µg g^{-1} TOC, Fig. 6a). At 19 of 20 sites, the *n*-alkanes showed a clear odd-over-even preference, reflected by a CPI ranging from 2.3-6.8, pointing to a predominant higher plant origin. The only exception was again the most western shelf site, where the CPI was 0.8. The ACL slightly varied between 29.4-30.4, without a spatial trend.

https://doi.org/10.5194/bg-2022-181
Preprint. Discussion started: 15 September 2022

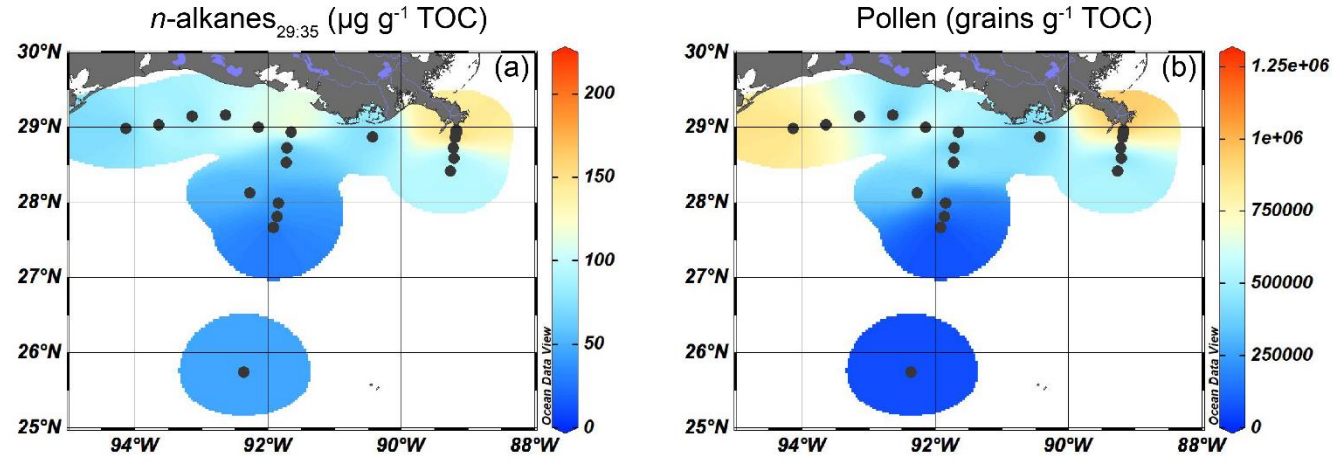

Figure 6: Isosurface plots for the input of higher plant-derived OM in surface sediments of the GoM, based on OC-normalized concentrations of a) long-chain (C_{29}-C_{35}) *n*-alkanes and b) pollen grains (excluding *Pinus* pollen).

4.3 Palynology

All sediments contained well-preserved marine (dinocysts) and terrestrial (pollen, spores) palynomorphs. The total dinocyst concentration was highest on the shelf and shallow Atchafalaya transect (<100 m, ~$5.0*10^5$ cysts g^{-1} TOC), and lowest along the Mississippi transect (~ $1.0*10^5$ cysts g^{-1} TOC) and the deeper part of the Atchafalaya transect (>100 m, ~$0.4 – 1.1*10^5$ cysts g^{-1} TOC, Fig. 7). In sediments close to the shelf and the MR, heterotrophic taxa dominated the assemblages (60-85% of total cysts), while autotrophic taxa were relatively more abundant in sediments from the open ocean (69-80%, Fig. 7).

Pollen and spores were most abundant close to the MR mouth (1.2 10^6 pollen g^{-1} TOC) and on the westernmost part of the shelf (8.8 10^5 pollen g^{-1} TOC, Fig. 6b). Their concentration decreased with increasing distance from the coast and reached a minimum of 3.9 10^4 pollen g^{-1} TOC at the deeper Atchafalaya transect.

https://doi.org/10.5194/bg-2022-181
Preprint. Discussion started: 15 September 2022

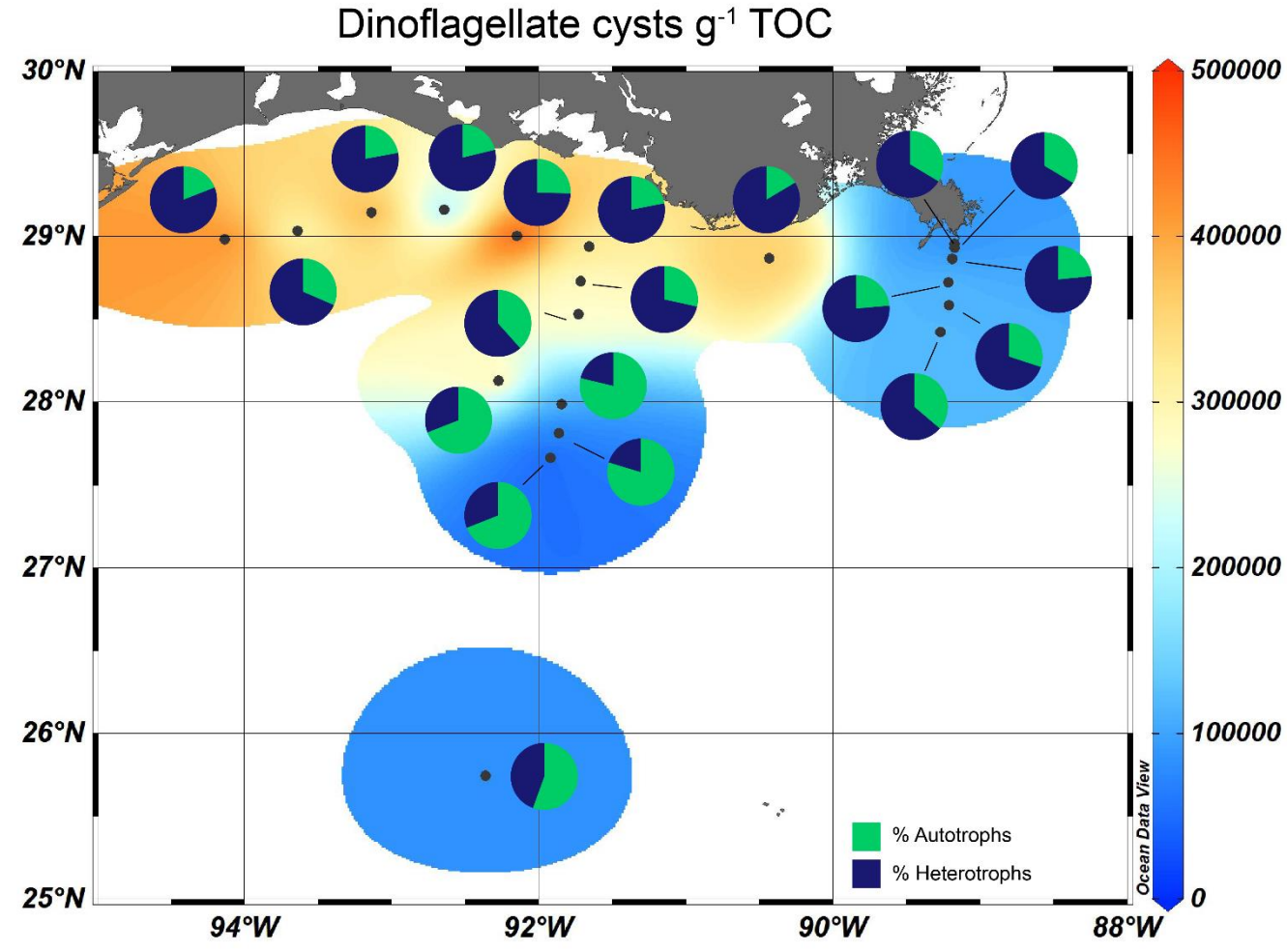

Figure 7: Isosurface plots of the TOC-normalized dinocyst concentration in GoM surface sediments overlain by pie-charts showing the contribution of autotroph and heterotroph species.

4.4 Statistical analysis on biomarker and palynology concentrations

The PCA of normalized biomarker, pollen, and dinoflagellate cyst concentrations in the surface sediments showed a variance of 55.6% on PC1 and 19.7% on PC2 (Fig. 8). Almost all variables plot positively on PC1, together with shallow shelf (<20 m water depth) sediments. The only exception is the concentration of alkenones, which plot negatively on PC1, with sediments at intermediate water depth (<80 m) on the Atchafalaya transect. Sediments from the deeper parts of the Mississippi (>50 m) and Atchafalaya (>200 m) transects also plot negative on PC1. PC2 mostly separates terrestrial and marine markers; the concentrations of *n*-alkanes, pollen and brGDGTs that are all considered to reflect a higher plant or soil source plot positively, while the concentrations of marine biomarkers alkenones, crenarchaeol, and 1,14-diols plot negatively. The sterols and the C_{32} 1,15-diols have generally low scores on this PC. Sediments from the MR transect scored

https://doi.org/10.5194/bg-2022-181
Preprint. Discussion started: 15 September 2022

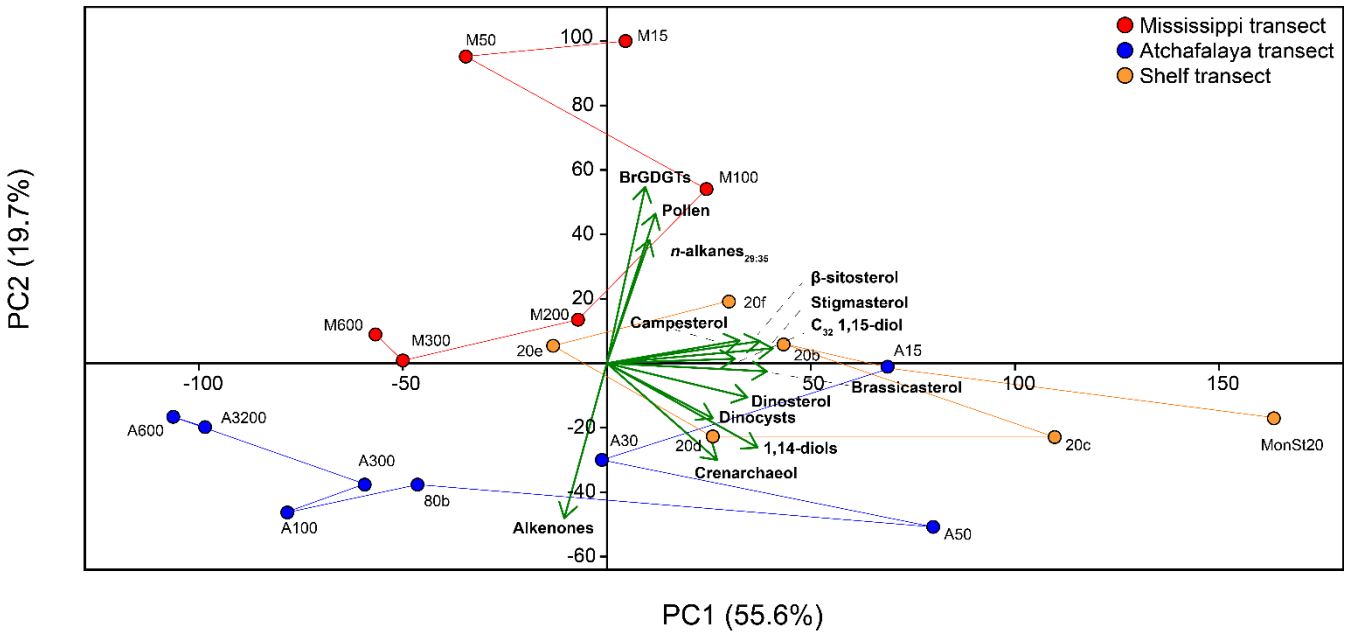

Figure 8: PCA on concentrations of brGDGTs, pollen, *n*-alkanes$_{29:35}$, campesterol, β-sitosterol, stigmasterol, the C_{32} 1,15-diol, brassicasterol, dinosterol, dinocysts, 1,14-diols, crenarchaeol and alkenones in surface sediments of the GoM. Lines connecting sample locations represent the scores of the different transects.

positively on PC2, while the AR transect scored negative on PC2. Sediments from the shelf transect have generally low scores on this PC.

5 Discussion

5.1 Spatial patterns of bulk OM parameters in surface sediments

The TOC content ranges from 0.7-1.6 wt.% on the MR and AR transects (Fig. 2a) but is substantially lower (0.05-0.53 wt.%) on the shelf transect, likely due to their sandy nature. In the studied surface sediments, the C/N ratio ranges from 8 to 12 (Fig. 2b), suggesting that the OM has a primarily marine origin, as the C/N ratio of marine OM typically ranges between 6-7, while the C/N ratios of terrestrial plant OM is >20 (Hedges et al., 1997). Close to the MR, the C/N ratio has its highest values, similar to the molar C/N ratio of 12.2 reported earlier for the MR delta (Bianchi et al., 2002).

The $\delta^{13}C_{org}$ values in the northern GoM are more negative close to the MAR and on the shelf (<-22.6‰, Fig. 2c), while they are more positive further offshore. While the $\delta^{13}C_{org}$ signature of C_3 higher plants, soils and freshwater algae ranges from ~-27‰ – -30‰, C_4 plants and marine algae have $\delta^{13}C_{org}$ values of ~-15‰ and ~-21‰, respectively (O'Leary, 1981; Hedges et al., 1997). The $\delta^{13}C_{org}$ values in the GoM thus show a predominant marine signal, especially further offshore. However, contributions of TerrOM such as C_4 plants could also be incorporated in this signal. For example, the distribution of lignin phenols in sediments of the Gulf of Mexico (GoM) showed that C_4 plant material was transported further offshore and

https://doi.org/10.5194/bg-2022-181
Preprint. Discussion started: 15 September 2022

contributed to the OM-pool in areas with enriched $\delta^{13}C_{org}$ signatures (Goñi et al., 1997, 1998; Bianchi et al., 2002). If $\delta^{13}C_{org}$ values alone would be used, this would have conventionally been interpreted as indicating a predominant marine origin of the OM. Therefore, it is important to further disentangle the sources of OM in the surface sediments, for which we here employed lipid biomarkers, pollen and dinocysts.

5.2 Sources and dispersal of fluvially discharged TerrOM

5.2.1 OM produced in freshwater

The input of fluvially produced OM into the northern GoM can be traced using the fractional abundance of the C_{32} 1,15-diol ($F_{C32\ 1,15}$), which is predominantly produced in freshwater, relative to that of the other 1,13- and 1,15 long-chain diols that have a marine origin (Lattaud et al., 2017, 2021). The $F_{C32\ 1,15}$ is highest proximal to the MR (50%) and decreases to <5% further offshore (Fig 5b). To assess whether the trend in $F_{C32\ 1,15}$ is driven by a marine overprint or a progressive loss of the C_{32} 1,15-diol upon river discharge, the trend in the sedimentary concentration of C_{32} 1,15-diol was evaluated. Interestingly, the highest TOC-normalized concentration of the C_{32} 1,15-diol is observed in sediments on the shelf west of the MR mouth, where $F_{C32\ 1,15}$ is low (Fig. 5). A possible explanation for this could be a westward transport of the C_{32} 1,15-diols combined with a substantial marine production of C_{28} and C_{30} 1,13- and 1,15-diols that overprint the C_{32} 1,15-diol concentrations, generating the low $F_{C32\ 1,15}$. In the PCA, the C_{32} 1,15-diols score in between terrestrial (brGDGTs, *n*-alkanes) and marine (alkenones, crenarchaeol) proxies on PC2 (Fig. 8), suggesting a mixed origin of fluvial and marine sources. However, previous studies have shown that marine production of the C_{32} 1,15-diol occurs in much smaller relative abundances than of the other long-chain diols and that the C_{32} 1,15-diol is predominantly produced in freshwater or brackish environments (Rampen et al., 2014b; Lattaud et al., 2017). Moreover, hydrogen isotopes of the C_{32} 1,15-diols from surface sediments in the northern GoM are more depleted close to the MAR, showing additional evidence of a freshwater source of the C_{32} 1,15-diols (Lattaud et al., 2019). Thus, the spatial pattern the C_{32} 1,15-diols with high abundances on the shelf and their position in the PCA plot suggests that that they are not immediately lost upon discharge, but are transported with the river plume along the shelf upon discharge. However, a marine contribution cannot be excluded based on the PCA results.

5.2.2 Soil-derived OC

An indication of the relative input of fluvially discharged soil OM may be provided by the BIT index (Hopmans et al., 2004). Only the two sites closest to the MR mouth have BIT index values >0.3, while the BIT index is always ≤0.1 for all other sites (Fig. 3b). The interpretation of the BIT index as a proxy for terrestrial OM input requires caution, as brGDGTs may also be produced in the coastal sediments and/or water column (e.g., Peterse et al., 2009; Xie et al., 2014; Sinninghe Damsté, 2016) and in rivers and lakes (Zell et al., 2013; De Jonge et al., 2014a; Weber et al., 2018). To assess the source(s) of brGDGTs in the northern GoM, the fractional abundances of tetra-, penta- and hexamethylated brGDGTs were plotted on a ternary diagram and compared to the position of global soils and peats (Fig. 9a; Dearing Crampton-Flood et al., 2019). A

https://doi.org/10.5194/bg-2022-181
Preprint. Discussion started: 15 September 2022

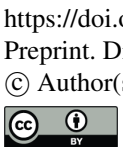

405 contribution of in situ produced marine brGDGTs can be recognized by an offset from the global soils (Sinninghe Damsté, 2016). The sediments collected close to the MR and along the shelf transect plot within the cloud of datapoints formed by the soils from the global dataset. This supports the idea that the sediments characterized by the high BIT index (>0.3) receive a substantial brGDGT influx form erosion of soil. On the other hand, sediments collected along the AR transect plot away from the cloud of data points formed by the global soil dataset. This is a clear indication that the brGDGTs at these sites are
410 not exclusively soil-derived. Indeed, brGDGTs in sediments that are offset from the global soils are also characterized by a #rings$_{tetra}$ of 0.37-0.91 (mean of 0.59 ± 0.17 SD, Fig 9b), which is significantly higher than the #rings$_{tetra}$ reported for global soils (0.21 ± 0.20 SD) and soils from the Mississippi catchment (0.23 ± 0.20 SD, n=14; De Jonge et al., 2014a), clearly indicating contributions of sedimentary in situ production (cf. Sinninghe Damsté, 2016). High #rings$_{tetra}$ of >0.7 on the western shelf and on the Atchafalaya transect in the zone between 30-300 m water depth indicates that most production of
415 brGDGTs takes place in situ (Fig. 9b). This matches the findings from other shelf areas, where in situ brGDGT production is most pronounced at 50-300 m water depth (e.g. Sinninghe Damsté, 2016; Ceccopieri et al., 2019).

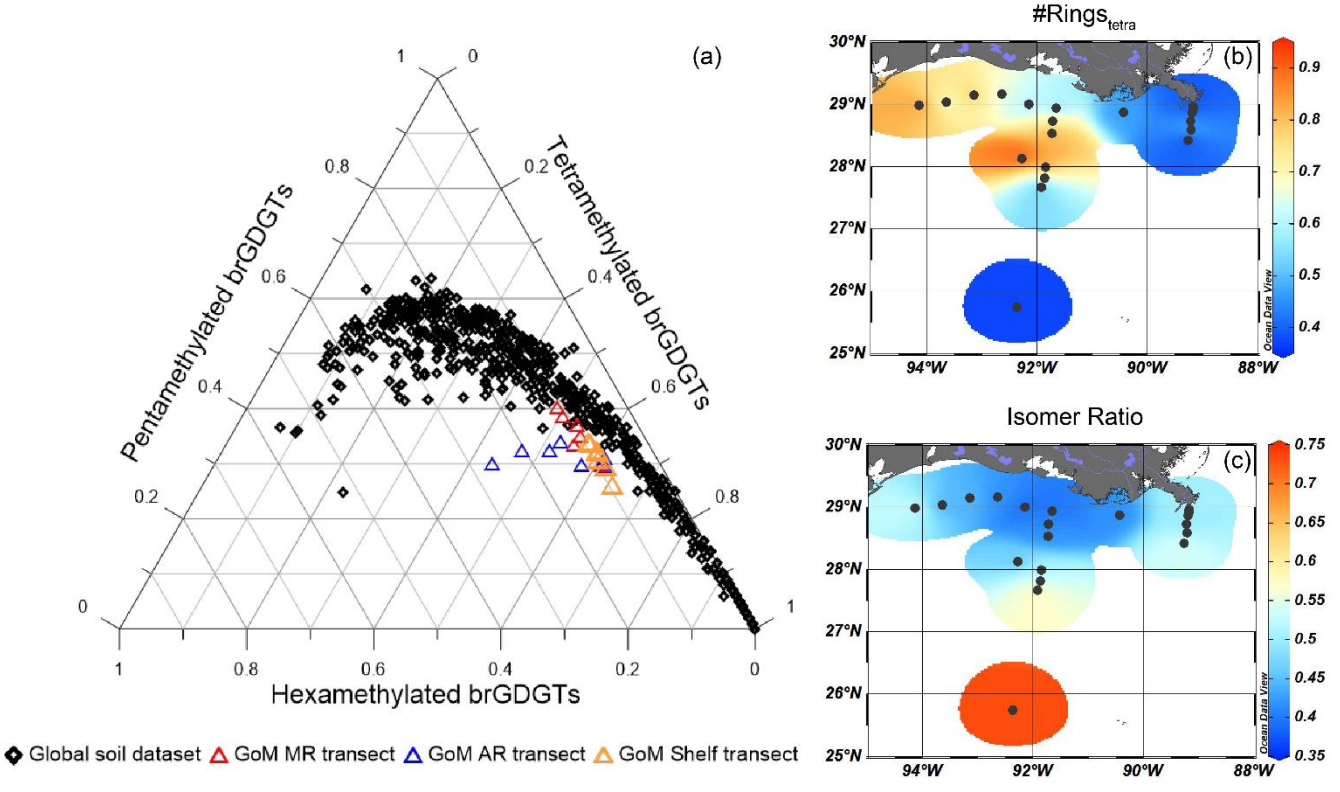

Figure 9: Assessment of the sources of brGDGTs in GoM surface sediments. A) Ternary diagram showing the tetra-, penta-, and
420 **hexamethylated brGDGTs in GoM surface sediments plotted together with the global soil and peat dataset (Dearing Crampton-Flood et al., 2019), b) the #rings$_{tetra}$, an indicator for marine produced brGDGTs and c) the Isomer Ratio (IR), indicative for fluvially produced brGDGTs.**

https://doi.org/10.5194/bg-2022-181
Preprint. Discussion started: 15 September 2022

Despite the sedimentary in situ contribution to the total pool of brGDGTs in this zone, the total brGDGT concentration is substantially lower than the crenarchaeol concentration, which results in a low BIT index. Close to the MR, where BIT index values are >0.3, the $\#rings_{tetra}$ ranges between 0.38-0.40. Although this is still slightly higher than the $\#rings_{tetra}$ from soils in the catchment area of the MR, the $\#rings_{tetra}$ close to the MR is substantially lower than elsewhere on the shelf, suggesting that the brGDGTs deposited close to the MR are predominantly soil-derived. Studies on the Yangtze, Tagus/Douro and Berau rivers have also reported high $\#rings_{tetra}$ in shelf regions (Zhu et al., 2011; Zell et al., 2015; Sinninghe Damsté, 2016). In these studies, a high $\#rings_{tetra}$ corresponded to rather low BIT index values, whereas in locations where the BIT index was high, a lower $\#rings_{tetra}$ was observed, indicating that the contribution of in situ produced brGDGTs on the BIT index was trivial.

Fluvially produced brGDGTs can be identified by the relative abundance of 6-methyl brGDGTs, quantified with the IR. This is based on the finding that the IR can be higher for brGDGTs in river suspended matter and sediments than in those in the catchment soils. This is likely due to the pH of river water that is generally higher than that of soils, thus promoting the production of 6-methyl brGDGTs in river waters that will also transport soil-derived GDGTs (De Jonge et al., 2014a). For example, brGDGT-based pH estimates for suspended particulate matter in the Yenisei river were much higher than that of the surrounding soils, which indicates an in situ contribution of brGDGTs, and was reflected by high IR values of >0.7 (De Jonge et al., 2014a).

While the pH of MR water is 8.2 (data from USGS at St. Francisville, Louisiana https://www.epa.gov/waterdata/water-quality-data#legacy), pH values of soils in the river catchment range from 5-8 (Slessarev et al., 2016). With the generally higher pH in the river compared to soils, fluvially produced brGDGTs are thus expected to have a higher IR. However, soils in the Mississippi catchment have an average IR of 0.43 ± 0.15 SD, n=14 (soil pH = 6.20 ± 0.86 SD) (De Jonge et al., 2014a), which is similar to the range in the Mississippi transect (0.49-0.55, Fig. 9c). Therefore, a freshwater contribution to the brGDGT pool in these sediments seems insignificant. The high IR in deeper (>3000 m) waters is unlikely to be the result of river input but rather by an increased amount of the brGDGT IIIa′ (Xu et al., 2020).

Close to the MR the brGDGT concentration and the BIT index are higher (>0.3) than in all other sediments. Since lacustrine in situ contribution is not evident, this indicates that the BIT index provides a realistic reflection of the fate of soil OM in the northern GoM.

The stark decrease in the BIT index in the off-shore transects indicate that most of the soil-derived brGDGTs are deposited in the sediments close to the river mouth. If we can use brGDGTs as a tracer for soil OM as a whole, this suggests that soil OM is not transported far after discharge. However, the BIT index is based on relative abundances of marine and terrestrial OM contributions, and a large contribution of marine OM may mask the terrestrial component. Normalizing the concentration of brGDGTs on TOC, however, reveals the same spatial pattern as that of the BIT index (Fig. 3), implying that soil-derived brGDGTs are probably not transported far into the marine realm, and are either directly transferred to the sediment or are rapidly lost after discharge into the GoM.

https://doi.org/10.5194/bg-2022-181
Preprint. Discussion started: 15 September 2022

The BIT index marks a starker decrease of soil material after discharge than the $F_{C32\ 1,15}$ of fluvial material, although the spatial pattern of the $F_{C32\ 1,15}$ resembles that of the BIT index ($r = 0.71$, $p < 0.005$) and the brGDGT concentration ($r = 0.89$, $p<0.005$, Fig. 3 and 5). If we assume that soil-derived brGDGTs and river-produced diols are appropriate tracers for soil- and fluvial OM as a whole, this suggests that fluvial OM may be transported further onto the shelf than soil-derived OM. Soil OM is generally assumed to form associations with mineral surfaces, which would protect this OM from degradation during land-sea transport (Mayer, 1994a, b; Keil et al., 1997). However, several studies have shown that OM appears to be progressively lost from mineral surfaces further offshore (Keil et al., 1997; Hou et al., 2020). During the transition from river to ocean, TerrOM might be replaced by marine OM due to the higher concentration of ions in seawater. Furthermore, TerrOM might be subjected to several cycles of deposition and erosion, causing TerrOM to transition between particulate and dissolved phases (Middelburg and Herman, 2007), which removes TerrOM from mineral surfaces. At this freshwater/salt water interface, flocculation of clay minerals may occur, which results in the sedimentation and thus loss of OM out of the water column (Sholkovitz, 1976). However, the brGDGT concentrations decrease more rapidly than other TerrOM sources. Possibly, due to the hydrophobic nature of brGDGTs, they could potentially form colloids rather than moving to the dissolved phase (Kirkels et al., 2022). Studies on brGDGTs in rivers have shown that their composition is stable throughout the water column, i.e. there is no preferential loss or production of a certain isomer, whereas the grain size and mineral composition are clearly depth segregated (Feng et al., 2016; Kirkels et al., 2020). This suggests that either their bonds with mineral surfaces are continuously renewed during transport, or that they are present in the form of colloids. After discharge, these colloids might then stay in seawater or degrade, which would explain their limited dispersal in the GoM sediments.

5.2.3 Higher plant-derived OC

We used long chain *n*-alkanes, pollen and spores in the surface sediments to trace higher plant OM input into the GoM. Here, we also discuss the use of stigmasterol, campesterol and β-sitosterol as indicators for higher plants, as these are also produced by higher plants (Volkman, 1986; Lütjohann, 2004). The plant markers are most abundant close to the MR mouth, where the highest concentrations of *n*-alkanes and pollen grains can be found, and on the shelf, where sterol concentrations peak (Fig 4, Fig. 6). The higher concentrations of higher plant markers on the shelf, matches that of the depleted $\delta^{13}C_{org}$ values (<-23‰) in this zone (Fig. 2c), suggesting that higher plant material may provide a substantial contribution to the TerrOM pool buried in the surface sediments.

Despite their shared higher plant source, all plant OM tracers show a distinct spatial pattern. For example, *n*-alkanes are present on the entire shelf transect (Fig. 6a), while pollen grains are most abundant close to the MR and on the westernmost shelf (Fig. 6c), where the proximity of extensive marshlands and river transport to Galveston Bay (Texas) might represent a secondary source for pollen. The presence of *n*-alkanes has also been observed in the central GoM, approximately 500 km south of the MR mouth (Tipple and Pagani, 2010), indicating that these biomarkers can be transported for long distances. Pollen and *n*-alkanes can be transported by both fluvial and aeolian transport pathways, but due to the large input of

https://doi.org/10.5194/bg-2022-181
Preprint. Discussion started: 15 September 2022

sediments and freshwater from the MAR into the northern GoM, we assume that the MAR is likely the dominant mode of transport of *n*-alkanes and pollen coming from the mainland US.

The relative abundance of stigmasterol, campesterol and β-sitosterol also varies spatially in the GoM; the fractional abundance of stigmasterol and campesterol is highest in shallow sediments close to the MR mouth and on the shelf in the reach from the river plume, whereas β-sitosterol is more dominant towards the open ocean (Fig. 4e,h,i). Since these sterols have additional microalgal sources, a critical evaluation of their origin is needed. β-sitosterol is the most dominant sterol in higher plants (Lütjohann, 2004), and in areas receiving large TerrOM inputs, it usually has a predominant higher plant origin (Yunker et al., 1995). In the northern GoM, β-sitosterol is consistently the most abundant higher plant-associated sterol in the sediments. However, the PCA that was performed on all biomarker, pollen, and dinoflagellate cyst concentrations, shows that all sterols have a low score on PC1 and plot in between the terrestrial and marine groups (Fig. 8). The similar response of all sterols indicate that they have common sources, although the presumed higher plant-derived sterols plot on the 'terrestrial side' of PC1, and the sterols derived from marine algae in the direction of other marine markers. Nevertheless, the different PCA results for pollen, *n*-alkanes and these sterols imply that the here considered sterols include an substantial algal contribution and are not solely derived from higher plants. Thus, pollen and *n*-alkanes may be more robust tracers of plant material input.

The spatial distribution of plant markers is also clearly different from those representing soil and freshwater OC, which were constrained to the MR mouth and nearby shelf (Fig 3, 5). Earlier studies have suggested that the transport of plant markers is sensitive to hydrodynamic processes in the coastal zone due to their association with mineral particles. Molecular plant markers associated with clay particles can be transported further into the open ocean than plant remains, which are usually associated with coarser grains (Goñi et al., 1997, 1998). The spatial distribution of plant-OM in the GoM shows that, in particular, *n*-alkanes could be preferentially associated with clay particles and thereby transported further off- and along shore, as these mineral associations not only facilitate their transport, but also provides protection from degradation (Mayer, 1994a, b; Keil et al., 1997; Lalonde et al., 2012). Possibly, the plant markers have a higher affinity to bind with mineral surfaces than brGDGTs or C_{32} 1,15-diols, which may explain their more widespread occurrence and better preservation in the GoM.

5.3 Identification of specific niches for OM production

The previous sections illustrated that the composition of TerrOM varied substantially spatially. In this section, we investigate patterns of marine productivity and assess marine OM composition in surface sediments of the northern GoM and relate it to the different producers. Information on marine productivity can be useful in at least two ways. It helps evaluating the reliability of indices and proxies that are based on the relative contribution of the two types of OC, terrestrial and marine, such as the BIT and the C/N ratio. Additionally, the identification of the main producers of the marine OM at a certain location provides indication of the spatial distribution of those organisms in the modern system. Such information, applied to downcore sediments, allow to assess changes in the niches of the different marine producers through time. For this scope, we

https://doi.org/10.5194/bg-2022-181
Preprint. Discussion started: 15 September 2022

used various biomarkers and dinocysts. The marine markers (i.e., crenarchaeol, 1,14-diols, dinosterol) show the highest concentrations in the sediments of the shelf and the shallow part (<100 m water depth) of the Atchafalaya transect (Fig. 4). This pattern fits with the westward direction of the river plume over the shelf, confirming that marine production is triggered by the nutrients discharged from the MAR (e.g., Lohrenz et al., 1997). The high $\delta^{13}C_{org}$ and relatively low C/N ratio values on the shelf (Fig. 2) confirm substantial marine productivity and its contribution to sedimentary OM in this area. Marine production is relatively low around the mouth of the MR. This can be explained by the high sediment load of the MR that causes turbid waters, generating unfavourable conditions for marine primary producers as photosynthesis is limited by light penetration into the water column (Lohrenz et al., 1990).

The spatial distribution of the different marine productivity and OM markers in the sediments varies. For example, crenarchaeol produced by ammonia oxidizing Thaumarchaeota, is most abundant on the shelf (Fig. 4a), where nutrient concentrations are highest due to discharge by the MAR (Rabalais et al., 2002; Van Meter et al., 2018). This is also evident from the low C/N values (≤10) on the shelf that indicate a nitrogen surplus (Fig. 2c). The long-chain 1,14-diols also mainly occur in the shelf sediments under the influence of the river plume (Fig. 4b). These compounds are produced by *Proboscia* diatoms, which thrive in high-nutrient areas (Sinninghe Damsté et al., 2003), where silica brought by the river is abundant. In contrast to crenarchaeol and diols, alkenones are most abundant in sediments at a water depth of 30-300 m, further offshore (Fig. 4c). This is in agreement with the niche for alkenone-producing haptophytes that are mostly observed in more oligotrophic waters (e.g., Menschel et al., 2016) and hence occur further offshore than the diatoms. In the southwestern GoM, haptophytes were most abundant in the deep photic zone (50-100 m water depth, Baumann and Boeckel, 2013).

The marine sterols brassicasterol and dinosterol are again most abundant on the shelf, although their relative abundances show different patterns, as dinosterol has a higher abundance in deeper waters compared to brassicasterol (Fig. 4d-e). Brassicasterol is often a predominant sterol of diatoms (Rampen et al., 2010), although it has also been attributed to many groups of marine phytoplankton (e.g., Volkman, 2003). Dinosterol is primarily produced by dinoflagellates, both the autotrophic and the heterotrophic ones, but its production can vary remarkably depending on the species (Volkman et al., 1993; Amo et al., 2010). The relationship between dinosterol abundance and dinocyst concentrations is complex (e.g., Leblond and Chapman, 2002; Mouradian et al., 2007), since not all dinoflagellates make cysts and dinosterol is not produced by all dinoflagellates. This is illustrated here by the total dinocyst concentrations, which are, in contrast with the distribution of dinosterol, higher on the shelf and decrease towards the open ocean.

Dinocysts also allow us to zoom in on the food chain, as autotrophic and heterotrophic dinocysts represent primary and secondary producers, respectively. The autotrophic species are clearly dominant in sediments of the GoM outside the river plume, i.e., towards the open ocean, and sediments along the Atchafalaya transect, where the water depth is >80 m (Fig. 7). Here, waters are less turbid, and light can penetrate deeper. The heterotrophic taxa are not dependent on light availability but exclusively on OM availability for food (e.g., diatoms and other organic debris) and dominate on the shelf and the shallow parts of the Atchafalaya and Mississippi transect. Other studies on dinocyst assemblages in surface sediments in the GoM also find high dinocyst concentrations and a strong dominance of heterotrophic species on the Louisiana shelf (Price et al.,

https://doi.org/10.5194/bg-2022-181
Preprint. Discussion started: 15 September 2022

2018), while dinocyst further offshore are less abundant and the assemblages are generally dominated by autotrophic species (Limoges et al., 2013).

As stated above, the amount of oxygen is bottom waters and sediments plays a role in dinocyst preservation. Previous studies have shown that in well oxygenated waters, heterotrophic cysts are more prone to degradation than autotrophic ones (Zonneveld et al., 2010). Since our surface sediment dataset is partly located in a seasonally hypoxic zone, but also includes surface sediments from water that are well oxygenated year-round, the high percentages of heterotrophic species on the shelf could be biased by the seasonally lower oxygen concentrations. However, several studies have demonstrated that the concentrations of heterotrophic cysts do correspond with export productivity (Reichart and Brinkhuis, 2003; Zonneveld et al., 2009). Dinocyst concentrations in the GoM are highest close to shore, indicating that the concentrations of heterotrophic taxa still show their relative dominance here.

The dominance of heterotrophs close to the MR in combination with the limited transfer of soil- and river-derived OM after discharge suggests the occurrence of priming. The priming effect is based on the increased turnover of recalcitrant OM upon addition of a more labile OM-source (Löhnis, 1926; Kuzyakov et al., 2000). In the coastal marine environment, the addition of freshly produced algal OM to supposedly more refractory TerrOM may trigger an increase in the decomposition rate, whereby also the more recalcitrant fraction is remineralized (Guenet et al., 2010; Bianchi, 2011). Priming has not been widely studied in marine systems, but several studies have shown increased TerrOM mineralization after the addition of primary produced OM (e.g., van Nugteren et al., 2009; Gontikaki et al., 2015), although results on the magnitude of the priming effect in aquatic systems are inconsistent (Bengtsson et al., 2018; Gontikaki and Witte, 2019). In the GoM, the occurrence of priming would imply that especially soil- and freshwater-derived OM is remineralized in the presence of fresh marine OC, which could explain the limited dispersal of soil- and fluvial-derived OM after discharge.

https://doi.org/10.5194/bg-2022-181
Preprint. Discussion started: 15 September 2022

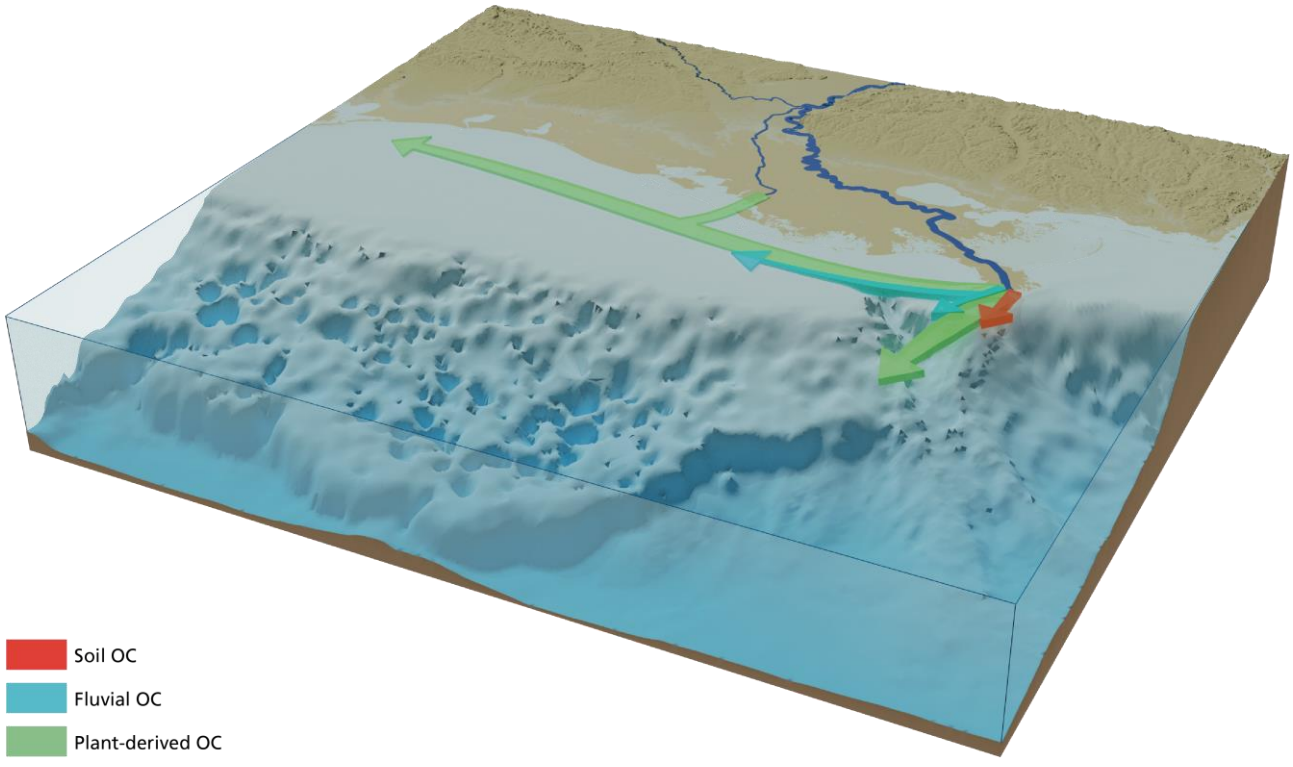

Fig 10. Schematic overview of the dispersal of soil-, fluvial- and higher plant-derived OC in the northern GoM based on the lipid biomarker, pollen, and dinocyst distributions from this study.

6 Conclusion

The biomarker and pollen distributions reveal that different types of TerrOM have distinct dispersal patterns upon discharge in the coastal zone (Fig. 10), where plant material reaches the deepest waters, while fluvial- and especially soil-derived OM are more confined to the proximity of the MR mouth. The distinct dispersal patterns of these different types of TerrOM can be linked to transport mechanisms and degradation processes. Soil-derived OM seems to be rapidly lost after discharge, either by forming colloids and subsequent dispersion in the water column or degraded due to priming, whereas plant markers are found further offshore associated with mineral surfaces, which protects them from degradation and facilitate their transport. The spatial variation in composition of the TerrOM in the GoM sediments implies that also the efficiency of coastal marine sediments as a long-term carbon sink is spatially variable. This has implications on the role of coastal zones as a hotspot for OM-burial, where mostly plant material has a higher burial efficiency on continental shelves.

Furthermore, the concentration of marine biomarkers and dinocysts in the surface sediments indicate that marine OM production is highest on the shelf. The spatial distribution of the biomarkers in the surface sediments reveals the preferred niches of the different marine producers, where dinoflagellates, diatoms, and Thaumarchaeota are found close to the coast, while coccolithophores are more present further offshore. In general, the shelf community is dominated by heterotrophic

dinoflagellate species, whereas autotrophic species occur in more oligotrophic waters further offshore. The dominance of heterotrophic dinocysts close to the MR mouth suggest that priming may have led to increased degradation of recalcitrant, mostly soil-derived TerrOM, limiting its dispersal further offshore. Our study thus shows that a detailed investigation on the composition of OM in marine continental margin sediments can reveal the processes that drive TerrOM distribution and burial in the marine environment.

Data statement

The dataset from this study is accessible through Pangaea (https://doi.pangaea.de/10.1594/PANGAEA.944838 (Yedema et al., 2022). The global soil and peat dataset is available at https://doi.org/10.1594/PANGAEA.907818 (Dearing Crampton-Flood et al., 2019).

Author contributions

FP and FS designed this study. FP and FS were involved in the sample collection. YWY performed the data analyses and wrote the manuscript together with all other co-authors. All co-authors provided feedback on the manuscript and contributed to the data interpretation.

Competing interests

The authors declare that they have no conflict of interest.

Acknowledgements

This work was carried out under the program of the Netherlands Earth System Science Centre (NESS), financially supported by the Dutch Ministry of Education, Culture and Science (OCW) (NESSC Gravitation Grant; grant no. 024.002.001). We thank Klaas Nierop, Desmond Eefting, Natasja Welters and Giovanni Dammers for their technical support. Thanks as well to all scientists and crew aboard the Pelagia cruise 64PE467.

References

Amo, M., Suzuki, N., Kawamura, H., Yamaguchi, A., Takano, Y., and Horiguchi, T.: Sterol composition of dinoflagellates: different abundance and composition in heterotrophic species and resting cysts, Geochem. J., 44, 225–231, https://doi.org/10.2343/geochemj.1.0063, 2010.

Aufdenkampe, A. K., Mayorga, E., Raymond, P. A., Melack, J. M., Doney, S. C., Alin, S. R., Aalto, R. E., and Yoo, K.: Riverine coupling of biogeochemical cycles between land, oceans, and atmosphere, Front. Ecol. Environ., 9, 53–60, https://doi.org/10.1890/100014, 2011.

Balzano, S., Lattaud, J., Villanueva, L., Rampen, S. W., Brussaard, C. P. D., van Bleijswijk, J., Bale, N., Sinninghe Damsté, J. S., and Schouten, S.: A quest for the biological sources of long chain alkyl diols in the western tropical North Atlantic Ocean, Biogeosciences, 15, 5951–5968, https://doi.org/10.5194/bg-15-5951-2018, 2018.

de Bar, M. W., Dorhout, D. J., Hopmans, E. C., Rampen, S. W., Damste, J. S. S., and Schouten, S.: Constraints on the application of long chain diol proxies in the Iberian Atlantic margin, Org. Geochem., 101, 184–195, https://doi.org/10.1016/j.orggeochem.2016.09.005, 2016.

Battin, T. J., Luyssaert, S., Kaplan, L. A., Aufdenkampe, A. K., Richter, A., and Tranvik, L. J.: The boundless carbon cycle, Nat. Geosci., 2, https://doi.org/10.1038/ngeo618, 2009.

Baumann, K.-H. and Boeckel, B.: Spatial distribution of living coccolithophores in the southwestern Gulf of Mexico, J. Micropalaeontology, 32, 123–133, https://doi.org/10.1144/jmpaleo2011-007, 2013.

Bengtsson, M. M., Attermeyer, K., and Catalán, N.: Interactive effects on organic matter processing from soils to the ocean: are priming effects relevant in aquatic ecosystems?, Hydrobiologia, 822, 1–17, https://doi.org/10.1007/s10750-018-3672-2, 2018.

Bianchi, T. S.: The role of terrestrially derived organic carbon in the coastal ocean: A changing paradigm and the priming effect, Proc. Natl. Acad. Sci., 108, 19473–19481, https://doi.org/10.1073/pnas.1017982108, 2011.

Bianchi, T. S. and Allison, M. A.: Large-river delta-front estuaries as natural "recorders" of global environmental change, Proc. Natl. Acad. Sci. U. S. A., 106, 8085–8092, https://doi.org/10.1073/pnas.0812878106, 2009.

Bianchi, T. S., Mitra, S., and McKee, B. A.: Sources of terrestrially-derived organic carbon in lower Mississippi River and Louisiana shelf sediments: implications for differential sedimentation and transport at the coastal margin, Mar. Chem., 77, 211–223, https://doi.org/10.1016/S0304-4203(01)00088-3, 2002.

Bianchi, T. S., Cui, X., Blair, N. E., Burdige, D. J., Eglinton, T. I., and Galy, V.: Centers of organic carbon burial and oxidation at the land-ocean interface, Org. Geochem., 115, 138–155, https://doi.org/10.1016/j.orggeochem.2017.09.008, 2018.

Blair, N. E. and Aller, R. C.: The Fate of Terrestrial Organic Carbon in the Marine Environment, Annu. Rev. Mar. Sci., 4, 401–423, https://doi.org/10.1146/annurev-marine-120709-142717, 2012.

Bray, E. and Evans, E.: Distribution of n-paraffins as a clue to recognition of source beds, Geochim. Cosmochim. Acta, 22, 2–15, https://doi.org/10.1016/0016-7037(61)90069-2, 1961.

van Bree, L. G., Peterse, F., Baxter, A. J., De Crop, W., Van Grinsven, S., Villanueva, L., Verschuren, D., and Sinninghe Damsté, J. S.: Seasonal variability and sources of in situ brGDGT production in a permanently stratified African crater lake, Biogeosciences, 17, 5443–5463, https://doi.org/10.5194/bg-17-5443-2020, 2020.

Burdige, D. J.: Burial of terrestrial organic matter in marine sediments: A re-assessment, Glob. Biogeochem. Cycles, 19, 1–7, https://doi.org/10.1029/2004GB002368, 2005.

Ceccopieri, M., Carreira, R. S., Wagener, A. L., Hefter, J., and Mollenhauer, G.: Branched GDGTs as proxies in surface sediments from the south-eastern Brazilian continental margin, Front. Earth Sci., 291, https://doi.org/10.3389/feart.2019.00291, 2019.

Chmura, G. L., Smirnov, A., and Campbell, I. D.: Pollen transport through distributaries and depositional patterns in coastal waters, Palaeogeogr. Palaeoclimatol. Palaeoecol., 149, 257–270, https://doi.org/10.1016/S0031-0182(98)00205-3, 1999.

Cole, J. J., Prairie, Y. T., Caraco, N. F., McDowell, W. H., Tranvik, L. J., Striegl, R. G., Duarte, C. M., Kortelainen, P., Downing, J. A., Middelburg, J. J., and Melack, J.: Plumbing the Global Carbon Cycle: Integrating Inland Waters into the Terrestrial Carbon Budget, Ecosystems, 10, 172–185, https://doi.org/10.1007/s10021-006-9013-8, 2007.

Coleman, J., Prior, D., and Lindsay, J. F.: Formation of Mississippi Canyon, AAPG Bull., 66, 1427–1428, https://doi.org/10.1306/03b5a80e-16d1-11d7-8645000102c1865d, 1982.

Corbett, D. R., McKee, B., and Allison, M.: Nature of decadal-scale sediment accumulation on the western shelf of the Mississippi River delta, Cont. Shelf Res., 26, 2125–2140, https://doi.org/10.1016/j.csr.2006.07.012, 2006.

De Jonge, C., Stadnitskaia, A., Hopmans, E. C., Cherkashov, G., Fedotov, A., and Sinninghe Damsté, J. S.: In situ produced branched glycerol dialkyl glycerol tetraethers in suspended particulate matter from the Yenisei River, Eastern Siberia, Geochim. Cosmochim. Acta, 125, 476–491, https://doi.org/10.1016/j.gca.2013.10.031, 2014a.

De Jonge, C., Hopmans, E. C., Zell, C. I., Kim, J.-H., Schouten, S., and Sinninghe Damsté, J. S.: Occurrence and abundance of 6-methyl branched glycerol dialkyl glycerol tetraethers in soils: Implications for palaeoclimate reconstruction, Geochim. Cosmochim. Acta, 141, 97–112, https://doi.org/10.1016/j.gca.2014.06.013, 2014b.

De Jonge, C., Kuramae, E. E., Radujković, D., Weedon, J. T., Janssens, I. A., and Peterse, F.: The influence of soil chemistry on branched tetraether lipids in mid-and high latitude soils: Implications for brGDGT-based paleothermometry, Geochim. Cosmochim. Acta, 310, 95–112, https://doi.org/10.1016/j.gca.2021.06.037, 2021.

Dearing Crampton-Flood, E., Tierney, J., Peterse, F., Kirkels, F., and Sinninghe Damsté, J.: Global soil and peat branched GDGT compilation dataset, PANGAEA Data Set, 10, https://doi.org/10.1016/j.gca.2019.09.043, 2019.

Deegan, L. A., Day Jr, J. W., Gosselink, J. G., Yáñez-Arancibia, A., Chavez, G. S., and Sanchez-Gil, P.: Relationships among physical characteristics, vegetation distribution and fisheries yield in Gulf of Mexico estuaries, in: Estuarine variability, Elsevier, 83–100, 1986.

Donders, T. H., Van Helmond, N. A., Verreussel, R., Munsterman, D., ten Veen, J., Speijer, R. P., Weijers, J. W., Sangiorgi, F., Peterse, F., and Reichart, G.-J.: Land–sea coupling of early Pleistocene glacial cycles in the southern North Sea exhibit dominant Northern Hemisphere forcing, Clim. Past, 14, 397–411, https://doi.org/10.5194/cp-14-397-2018, 2018.

Eglinton, G. and Hamilton, R.: The distribution of alkanes, in: Chemical plant taxonomy, vol. 187, Academic Press, Inc., New York, NY, 217, https://doi.org/10.1016/B978-0-12-395540-1.50012-9, 1963.

Feng, X., Feakins, S. J., Liu, Z., Ponton, C., Wang, R. Z., Karkabi, E., Galy, V., Berelson, W. M., Nottingham, A. T., and Meir, P.: Source to sink: Evolution of lignin composition in the Madre de Dios River system with connection to the Amazon basin and offshore, J. Geophys. Res. Biogeosciences, 121, 1316–1338, https://doi.org/10.1002/2016JG003323, 2016.

Gagosian, R. B., Peltzer, E. T., and Merrill, J. T.: Long-range transport of terrestrially derived lipids in aerosols from the South Pacific, Nature, 325, 800–803, https://doi.org/10.1038/325800a0, 1987.

Gaines, G. and Taylor, F.: Extracellular digestion in marine dinoflagellates, J. Plankton Res., 6, 1057–1061, https://doi.org/10.1093/plankt/6.6.1057, 1984.

Goñi, M. A., Ruttenberg, K. C., and Eglinton, T. I.: Sources and contribution of terrigenous organic carbon to surface sediments in the Gulf of Mexico, Nature, 389, 275–278, https://doi.org/10.1038/38477, 1997.

Goñi, M. A., Ruttenberg, K. C., and Eglinton, T. I.: A reassessment of the sources and importance of land-derived organic matter in surface sediments from the Gulf of Mexico, Geochim. Cosmochim. Acta, 62, 3055–3075, https://doi.org/10.1016/S0016-7037(98)00217-8, 1998.

Gontikaki, E. and Witte, U.: No strong evidence of priming effects on the degradation of terrestrial plant detritus in estuarine sediments, Front. Mar. Sci., 6, 327, https://doi.org/10.3389/fmars.2019.00327, 2019.

Gontikaki, E., Thornton, B., Cornulier, T., and Witte, U.: Occurrence of priming in the degradation of lignocellulose in marine sediments, PLoS One, 10, e0143917, https://doi.org/10.1371/journal.pone.0143917, 2015.

Guenet, B., Danger, M., Abbadie, L., and Lacroix, G.: Priming effect: bridging the gap between terrestrial and aquatic ecology, Ecology, 91, 2850–2861, https://doi.org/10.1890/09-1968.1, 2010.

Hammer, Ø., Harper, D. A., and Ryan, P. D.: PAST: Paleontological statistics software package for education and data analysis, Palaeontol. Electron., 4, 9, https://doi.org/10.1002/9780470750711, 2001.

Hardy, W., Penaud, A., Marret, F., Bayon, G., Marsset, T., and Droz, L.: Dinocyst assemblage constraints on oceanographic and atmospheric processes in the eastern equatorial Atlantic over the last 44 kyr, Biogeosciences, 13, 4823–4841, https://doi.org/10.5194/bg-13-4823-2016, 2016.

Head, M.: Modern dinoflagellate cysts and their biological affinities, in: Palynology: principles and applications, vol. 3, 1197–1248, https://doi.org/10.2307/1485834, 1996.

Hedges, J. I., Keil, R. G., and Benner, R.: What happens to terrestrial organic matter in the ocean?, Org. Geochem., 27, 195–212, https://doi.org/10.1016/S0146-6380(97)00066-1, 1997.

Hedges, J. I., Hu, F. S., Devol, A. H., Hartnett, H. E., Tsamakis, E., and Keil, R. G.: Sedimentary organic matter preservation; a test for selective degradation under oxic conditions, Am. J. Sci., 299, 529–555, https://doi.org/10.2475/ajs.299.7-9.529, 1999.

Heusser, L. E.: Pollen distribution in marine sediments on the continental margin off northern California, Mar. Geol., 80, 131–147, https://doi.org/10.1016/0025-3227(88)90076-X, 1988.

https://doi.org/10.5194/bg-2022-181
Preprint. Discussion started: 15 September 2022

Hopmans, E. C., Weijers, J. W., Schefuß, E., Herfort, L., Sinninghe Damsté, J. S., and Schouten, S.: A novel proxy for terrestrial organic matter in sediments based on branched and isoprenoid tetraether lipids, Earth Planet. Sci. Lett., 224, 107–116, https://doi.org/10.1016/j.epsl.2004.05.012, 2004.

Hopmans, E. C., Schouten, S., and Sinninghe Damsté, J. S.: The effect of improved chromatography on GDGT-based palaeoproxies, Org. Geochem., 93, 1–6, https://doi.org/10.1016/j.orggeochem.2015.12.006, 2016.

Hou, P., Yu, M., Zhao, M., Montluçon, D. B., Su, C., and Eglinton, T. I.: Terrestrial Biomolecular Burial Efficiencies on Continental Margins, J. Geophys. Res. Biogeosciences, 125, https://doi.org/10.1029/2019JG005520, 2020.

Keil, R. G., Mayer, L. M., Quay, P. D., Richey, J. E., and Hedges, J. I.: Loss of organic matter from riverine particles in deltas, Geochim. Cosmochim. Acta, 61, 1507–1511, https://doi.org/10.1016/S0016-7037(97)00044-6, 1997.

Kirkels, F. M., Ponton, C., Galy, V., West, A. J., Feakins, S. J., and Peterse, F.: From Andes to Amazon: Assessing branched tetraether lipids as tracers for soil organic carbon in the Madre de Dios River system, J. Geophys. Res. Biogeosciences, 125, e2019JG005270, https://doi.org/10.1029/2019JG005270, 2020.

Kirschbaum, M. U. F., Zeng, G., Ximenes, F., Giltrap, D. L., and Zeldis, J. R.: Towards a more complete quantification of the global carbon cycle, Biogeosciences, 16, 831–846, https://doi.org/10.5194/bg-16-831-2019, 2019.

Koga, Y., Nishihara, M., Morii, H., and Akagawa-Matsushita, M.: Ether polar lipids of methanogenic bacteria: structures, comparative aspects, and biosyntheses, Microbiol. Rev., 57, 164–182, https://doi.org/10.1128/mr.57.1.164-182.1993, 1993.

Kuzyakov, Y., Friedel, J., and Stahr, K.: Review of mechanisms and quantification of priming effects, Soil Biol. Biochem., 32, 1485–1498, https://doi.org/10.1016/S0038-0717(00)00084-5, 2000.

Lalonde, K., Mucci, A., Ouellet, A., and Gélinas, Y.: Preservation of organic matter in sediments promoted by iron, Nature, 483, 198–200, https://doi.org/10.1038/nature10855, 2012.

Lattaud, J., Kim, J. H., De Jonge, C., Zell, C., Sinninghe Damsté, J. S., and Schouten, S.: The C32 alkane-1,15-diol as a tracer for riverine input in coastal seas, Geochim. Cosmochim. Acta, 202, 146–158, https://doi.org/10.1016/j.gca.2016.12.030, 2017.

Lattaud, J., Erdem, Z., Weiss, G. M., Rush, D., Balzano, S., Chivall, D., van der Meer, M. T., Hopmans, E. C., Damsté, J. S. S., and Schouten, S.: Hydrogen isotopic ratios of long-chain diols reflect salinity, Org. Geochem., 137, 103904, https://doi.org/10.1016/j.orggeochem.2019.103904, 2019.

Lattaud, J., Balzano, S., van der Meer, M. T., Villanueva, L., Hopmans, E. C., Sinninghe Damsté, J. S., and Schouten, S.: Sources and seasonality of long-chain diols in a temperate lake (Lake Geneva), Org. Geochem., 156, 104223, https://doi.org/10.1016/j.orggeochem.2021.104223, 2021.

Leblond, J. D. and Chapman, P. J.: A survey of the sterol composition of the marine dinoflagellates Karenia brevis, Karenia mikimotoi, and Karlodinium micrum distribution of sterols within other members of the class Dinophyceae, J. Phycol., 38, 670–682, https://doi.org/10.1046/j.1529-8817.2002.01181.x, 2002.

Li, M., Peng, C., Wang, M., Xue, W., Zhang, K., Wang, K., Shi, G., and Zhu, Q.: The carbon flux of global rivers: A re-evaluation of amount and spatial patterns, Ecol. Indic., 80, 40–51, https://doi.org/10.1016/j.ecolind.2017.04.049, 2017.

Limoges, A., Londeix, L., and de Vernal, A.: Organic-walled dinoflagellate cyst distribution in the Gulf of Mexico, Mar. Micropaleontol., 102, 51–68, https://doi.org/10.1016/j.marmicro.2013.06.002, 2013.

Löhnis, F.: Nitrogen availability of green manures, Soil Sci., 22, 253–290, https://doi.org/10.1097/00010694-192610000-00001, 1926.

Lohrenz, S. E., Dagg, M. J., and Whitledge, T. E.: Enhanced primary production at the plume/oceanic interface of the Mississippi River, Cont. Shelf Res., 10, 639–664, https://doi.org/10.1016/0278-4343(90)90043-L, 1990.

Lohrenz, S. E., Fahnenstiel, G. L., Redalje, D. G., Lang, G. A., Chen, X., and Dagg, M. J.: Variations in primary production of northern Gulf of Mexico continental shelf waters linked to nutrient inputs from the Mississippi River, Mar. Ecol. Prog. Ser., 155, 45–54, https://doi.org/10.3354/meps155045, 1997.

Lütjohann, D.: Sterol autoxidation: from phytosterols to oxyphytosterols, Br. J. Nutr., 91, 3–4, https://doi.org/10.1079/BJN20031048, 2004.

Marzi, R., Torkelson, B., and Olson, R.: A revised carbon preference index, Org. Geochem., 20, 1303–1306, https://doi.org/10.1016/0146-6380(93)90016-5, 1993.

Mayer, L. M.: Relationships between mineral surfaces and organic carbon concentrations in soils and sediments, Chem. Geol., 114, 347–363, https://doi.org/10.1016/0009-2541(94)90063-9, 1994a.

Mayer, L. M.: Surface area control of organic carbon accumulation in continental shelf sediments, Geochim. Cosmochim. Acta, 58, 1271–1284, https://doi.org/10.1016/0016-7037(94)90381-6, 1994b.

Mayorga, E., Aufdenkampe, A. K., Masiello, C. A., Krusche, A. V., Hedges, J. I., Quay, P. D., Richey, J. E., and Brown, T. A.: Young organic matter as a source of carbon dioxide outgassing from Amazonian rivers, Nature, 436, 538–541, https://doi.org/10.1038/nature03880, 2005.

Menschel, E., González, H. E., and Giesecke, R.: Coastal-oceanic distribution gradient of coccolithophores and their role in the carbonate flux of the upwelling system off Concepción, Chile (36°S), J. Plankton Res., 38, 798–817, https://doi.org/10.1093/plankt/fbw037, 2016.

Meyers, P. A.: Organic geochemical proxies of paleoceanographic, paleolimnologic, and paleoclimatic processes, Org. Geochem., 27, 213–250, https://doi.org/10.1016/S0146-6380(97)00049-1, 1997.

Middelburg, J. J. and Herman, P. M.: Organic matter processing in tidal estuaries, Mar. Chem., 106, 127–147, https://doi.org/10.1016/j.marchem.2006.02.007, 2007.

Milliman, J. D. and Syvitski, J. P. M.: Geomorphic/Tectonic Control of Sediment Discharge to the Ocean: The Importance of Small Mountainous Rivers, J. Geol., 100, 525–544, https://doi.org/10.1086/629606, 1992.

Mouradian, M., Panetta, R. J., De Vernal, A., and Gélinas, Y.: Dinosterols or dinocysts to estimate dinoflagellate contributions to marine sedimentary organic matter?, Limnol. Oceanogr., 52, 2569–2581, https://doi.org/10.4319/lo.2007.52.6.2569, 2007.

Mudie, P. J. and McCarthy, F. M. G.: Late quaternary pollen transport processes, western North Atlantic: Data from box models, cross-margin and N-S transects, Mar. Geol., 118, 79–105, https://doi.org/10.1016/0025-3227(94)90114-7, 1994.

Neill, C. F. and Allison, M. A.: Subaqueous deltaic formation on the Atchafalaya Shelf, Louisiana, Mar. Geol., 214, 411–430, https://doi.org/10.1016/j.margeo.2004.11.002, 2005.

van Nugteren, P., Moodley, L., Brummer, G.-J., Heip, C. H., Herman, P. M., and Middelburg, J. J.: Seafloor ecosystem functioning: the importance of organic matter priming, Mar. Biol., 156, 2277–2287, https://doi.org/10.1007/s00227-009-1255-5, 2009.

O'Leary, H.: Carbon isotope fractionation in plants, Phytochemistry, 20, 553–567, https://doi.org/10.1016/0031-9422(81)85134-5, 1981.

Peterse, F., Kim, J.-H., Schouten, S., Kristensen, D. K., Koç, N., and Sinninghe Damsté, J. S.: Constraints on the application of the MBT/CBT palaeothermometer at high latitude environments (Svalbard, Norway), Org. Geochem., 40, 692–699, https://doi.org/10.1016/j.orggeochem.2009.03.004, 2009.

Poynter, J., Farrimond, P., Robinson, N., and Eglinton, G.: Aeolian-derived higher plant lipids in the marine sedimentary record: Links with palaeoclimate, in: Paleoclimatology and paleometeorology: modern and past patterns of global atmospheric transport, Springer, 435–462, https://doi.org/10.1007/978-94-009-0995-3_18, 1989.

Price, A. M., Baustian, M. M., Turner, R. E., Rabalais, N. N., and Chmura, G. L.: Dinoflagellate Cysts Track Eutrophication in the Northern Gulf of Mexico, Estuaries Coasts, 41, 1322–1336, https://doi.org/10.1007/s12237-017-0351-x, 2018.

Rabalais, N. N. and Turner, R. E.: Gulf of Mexico hypoxia: Past, present, and future, Limnol. Oceanogr. Bull., 28, 117–124, https://doi.org/10.1002/lob.10351, 2019.

Rabalais, N. N., Turner, R. E., and Wiseman Jr, W. J.: Gulf of Mexico hypoxia, aka "The dead zone," Annu. Rev. Ecol. Syst., 33, 235–263, https://doi.org/10.1146/annurev.ecolsys.33.010802.150513, 2002.

Rabalais, N. N., Turner, R. E., Sen Gupta, B. K., Boesch, D. F., Chapman, P., and Murrell, M. C.: Hypoxia in the northern Gulf of Mexico: Does the science support the plan to reduce, mitigate, and control hypoxia?, Estuaries Coasts, 30, 753–772, https://doi.org/10.1007/BF02841332, 2007.

Rampen, S. W., Abbas, B. A., Schouten, S., and Sinninghe Damste, J. S.: A comprehensive study of sterols in marine diatoms (Bacillariophyta): Implications for their use as tracers for diatom productivity, Limnol. Oceanogr., 55, 91–105, https://doi.org/10.4319/lo.2010.55.1.0091, 2010.

Rampen, S. W., Willmott, V., Kim, J.-H., Uliana, E., Mollenhauer, G., Schefuß, E., Sinninghe Damsté, J. S., and Schouten, S.: Long chain 1,13- and 1,15-diols as a potential proxy for palaeotemperature reconstruction, Geochim. Cosmochim. Acta, 84, 204–216, https://doi.org/10.1016/j.gca.2012.01.024, 2012.

Rampen, S. W., Willmott, V., Kim, J.-H., Rodrigo-Gámiz, M., Uliana, E., Mollenhauer, G., Schefuß, E., Sinninghe Damsté, J. S., and Schouten, S.: Evaluation of long chain 1,14-alkyl diols in marine sediments as indicators for upwelling and temperature, Org. Geochem., 76, 39–47, https://doi.org/10.1016/j.orggeochem.2014.07.012, 2014a.

Rampen, S. W., Datema, M., Rodrigo-Gámiz, M., Schouten, S., Reichart, G.-J., and Sinninghe Damsté, J. S.: Sources and proxy potential of long chain alkyl diols in lacustrine environments, Geochim. Cosmochim. Acta, 144, 59–71, https://doi.org/10.1016/j.gca.2014.08.033, 2014b.

Regnier, P., Friedlingstein, P., Ciais, P., Mackenzie, F. T., Gruber, N., Janssens, I. A., Laruelle, G. G., Lauerwald, R., Luyssaert, S., Andersson, A. J., Arndt, S., Arnosti, C., Borges, A. V., Dale, A. W., Gallego-Sala, A., Goddéris, Y., Goossens, N., Hartmann, J., Heinze, C., Ilyina, T., Joos, F., LaRowe, D. E., Leifeld, J., Meysman, F. J. R., Munhoven, G., Raymond, P. A., Spahni, R., Suntharalingam, P., and Thullner, M.: Anthropogenic perturbation of the carbon fluxes from land to ocean, Nat. Geosci., 6, 597–607, https://doi.org/10.1038/ngeo1830, 2013.

Reichart, G.-J. and Brinkhuis, H.: Late Quaternary Protoperidinium cysts as indicators of paleoproductivity in the northern Arabian Sea, Mar. Micropaleontol., 49, 303–315, https://doi.org/10.1016/S0377-8398(03)00050-1, 2003.

Reid, P. C. and Harland, R.: Studies of Quaternary dinoflagellate cysts from the North Atlantic, Contrib. Stratigr. Palynol., 1, 147–169, 1977.

Reuss, M.: Designing the bayous: The control of water in the Atchafalaya Basin, 1800-1995, Texas A&M University Press, https://doi.org/10.2307/27649250, 2004.

Rochon, A., Vernal, A. de, Turon, J.-L., Matthiessen, J., and Head, M. J.: Distribution of recent dinoflagellate cysts in surface sediments from the North Atlantic Ocean and adjacent seas in relation to sea-surface parameters, Am. Assoc. Stratigr. Palynol. Contrib. Ser., 35, 1–146, https://doi.org/10013/epic.14283, 1999.

Rontani, J.-F., Charrière, B., Sempéré, R., Doxaran, D., Vaultier, F., Vonk, J. E., and Volkman, J. K.: Degradation of sterols and terrigenous organic matter in waters of the Mackenzie Shelf, Canadian Arctic, Org. Geochem., 75, 61–73, https://doi.org/10.1016/j.orggeochem.2014.06.002, 2014.

Sangiorgi, F. and Donders, T. H.: Reconstructing 150 years of eutrophication in the north-western Adriatic Sea (Italy) using dinoflagellate cysts, pollen and spores, Estuar. Coast. Shelf Sci., 60, 69–79, https://doi.org/10.1016/j.ecss.2003.12.001, 2004.

Sangiorgi, F., Fabbri, D., Comandini, M., Gabbianelli, G., and Tagliavini, E.: The distribution of sterols and organic-walled dinoflagellate cysts in surface sediments of the North-western Adriatic Sea (Italy), Estuar. Coast. Shelf Sci., 64, 395–406, https://doi.org/10.1016/j.ecss.2005.03.005, 2005.

Santschi, P. H. and Rowe, G. T.: Radiocarbon-derived sedimentation rates in the Gulf of Mexico, Deep Sea Res. Part II Top. Stud. Oceanogr., 55, 2572–2576, https://doi.org/10.1016/j.dsr2.2008.07.005, 2008.

Schlitzer, R.: Data analysis and visualization with Ocean Data View, CMOS Bull. SCMO, 43, 9–13, https://doi.org/10013/epic.45187, 2015.

Shimokawara, M., Nishimura, M., Matsuda, T., Akiyama, N., and Kawai, T.: Bound forms, compositional features, major sources and diagenesis of long chain, alkyl mid-chain diols in Lake Baikal sediments over the past 28,000 years, Org. Geochem., 41, 753–766, https://doi.org/10.1016/j.orggeochem.2010.05.013, 2010.

Sholkovitz, E.: Flocculation of dissolved organic and inorganic matter during the mixing of river water and seawater, Geochim. Cosmochim. Acta, 40, 831–845, 1976.

Sinninghe Damsté, J. S.: Spatial heterogeneity of sources of branched tetraethers in shelf systems: The geochemistry of tetraethers in the Berau River delta (Kalimantan, Indonesia), Geochim. Cosmochim. Acta, 186, 13–31, https://doi.org/10.1016/j.gca.2016.04.033, 2016.

Sinninghe Damsté, J. S., Hopmans, E. C., Pancost, R. D., Schouten, S., and Geenevasen, J. A.: Newly discovered non-isoprenoid glycerol dialkyl glycerol tetraether lipids in sediments, Chem. Commun., 1683–1684, https://doi.org/10.1039/B004517I, 2000.

Sinninghe Damsté, J. S., Schouten, S., Hopmans, E. C., Van Duin, A. C., and Geenevasen, J. A.: Crenarchaeol: The characteristic glycerol dibiphytanyl glycerol tetraether membrane lipid of cosmopolitan pelagic crenarchaeota, J. Lipid Res., 43, 1641–1651, https://doi.org/10.1194/jlr.M200148-JLR200, 2002.

Sinninghe Damsté, J. S., Rampen, S., Irene, W., Rijpstra, C., Abbas, B., Muyzer, G., and Schouten, S.: A diatomaceous origin for long-chain diols and mid-chain hydroxy methyl alkanoates widely occurring in Quaternary marine sediments: Indicators for high-nutrient conditions, Geochim. Cosmochim. Acta, 67, 1339–1348, https://doi.org/10.1016/S0016-7037(02)01225-5, 2003.

Sinninghe Damsté, J. S., Rijpstra, W. I. C., Hopmans, E. C., Weijers, J. W., Foesel, B. U., Overmann, J., and Dedysh, S. N.: 13, 16-Dimethyl octacosanedioic acid (iso-diabolic acid), a common membrane-spanning lipid of Acidobacteria subdivisions 1 and 3, Appl. Environ. Microbiol., 77, 4147–4154, https://doi.org/10.1128/AEM.00466-11, 2011.

Sinninghe Damsté, J. S., Rijpstra, W. I. C., Foesel, B. U., Huber, K. J., Overmann, J., Nakagawa, S., Kim, J. J., Dunfield, P. F., Dedysh, S. N., and Villanueva, L.: An overview of the occurrence of ether-and ester-linked iso-diabolic acid membrane lipids in microbial cultures of the Acidobacteria: Implications for brGDGT paleoproxies for temperature and pH, Org. Geochem., 124, 63–76, https://doi.org/10.1016/j.orggeochem.2018.07.006, 2018.

Slessarev, E., Lin, Y., Bingham, N., Johnson, J., Dai, Y., Schimel, J., and Chadwick, O.: Water balance creates a threshold in soil pH at the global scale, Nature, 540, 567–569, https://doi.org/10.1038/nature20139, 2016.

Stockmarr, J.: Tablets with spores used in absolute pollen analysis, Pollen Spores, 13, 615–621, 1971.

Sturges, W. and Evans, J.: On the variability of the Loop Current in the Gulf of Mexico, J. Mar. Res., 41, 639–653, https://doi.org/10.1357/002224083788520487, 1983.

Tipple, B. J. and Pagani, M.: A 35Myr North American leaf-wax compound-specific carbon and hydrogen isotope record: Implications for C4 grasslands and hydrologic cycle dynamics, Earth Planet. Sci. Lett., 299, 250–262, https://doi.org/10.1016/j.epsl.2010.09.006, 2010.

Tranvik, L. J., Downing, J. A., Cotner, J. B., Loiselle, S. A., Striegl, R. G., Ballatore, T. J., Dillon, P., Finlay, K., Fortino, K., Knoll, L. B., Kortelainen, P. L., Kutser, T., Larsen, Soren., Laurion, I., Leech, D. M., McCallister, S. L., McKnight, D. M., Melack, J. M., Overholt, E., Porter, J. A., Prairie, Y., Renwick, W. H., Roland, F., Sherman, B. S., Schindler, D. W., Sobek, S., Tremblay, A., Vanni, M. J., Verschoor, A. M., von Wachenfeldt, E., and Weyhenmeyer, G. A.: Lakes and reservoirs as regulators of carbon cycling and climate, Limnol. Oceanogr., 54, 2298–2314, https://doi.org/10.4319/lo.2009.54.6_part_2.2298, 2009.

Van Meter, K. J., Van Cappellen, P., and Basu, N. B.: Legacy nitrogen may prevent achievement of water quality goals in the Gulf of Mexico, Science, 360, 427–430, https://doi.org/10.1126/science.aar4462, 2018.

Volkman, J.: Sterols in microorganisms, Appl. Microbiol. Biotechnol., 60, 495–506, https://doi.org/10.1007/s00253-002-1172-8, 2003.

Volkman, J. K.: Sterols in microalgae, Physiol. Microalgae, 485–505, https://doi.org/10.1007/978-3-319-24945-2_19, 2016.

Volkman, J., Eglinton, G., Corner, E., and Sargent, J.: Novel unsaturated straight-chain C37-C39 methyl and ethyl ketones in marine sediments and a coccolithophore Emiliania huxleyi, Phys. Chem. Earth, 12, 219–227, https://doi.org/10.1016/0079-1946(79)90106-X, 1980.

Volkman, J. K.: A review of sterol markers for marine and terrigenous organic matter, Org. Geochem., 9, 83–99, https://doi.org/10.1016/0146-6380(86)90089-6, 1986.

Volkman, J. K., Barrett, S. M., Dunstan, G. A., and Jeffrey, S.: C30-C32 alkyl diols and unsaturated alcohols in microalgae of the class Eustigmatophyceae, Org. Geochem., 18, 131–138, https://doi.org/10.1016/0146-6380(92)90150-V, 1992.

Volkman, J. K., Barrett, S. M., Dunstan, G. A., and Jeffrey, S.: Geochemical significance of the occurrence of dinosterol and other 4-methyl sterols in a marine diatom, Org. Geochem., 20, 7–15, https://doi.org/10.1016/0146-6380(93)90076-N, 1993.

Warden, L., Kim, J.-H., Zell, C., Vis, G.-J., de Stigter, H., Bonnin, J., and Sinninghe Damsté, J. S.: Examining the provenance of branched GDGTs in the Tagus River drainage basin and its outflow into the Atlantic Ocean over the Holocene to determine their usefulness for paleoclimate applications, Biogeosciences, 13, 5719–5738, https://doi.org/10.5194/bg-13-5719-2016, 2016.

Weber, Y., Damsté, J. S. S., Zopfi, J., De Jonge, C., Gilli, A., Schubert, C. J., Lepori, F., Lehmann, M. F., and Niemann, H.: Redox-dependent niche differentiation provides evidence for multiple bacterial sources of glycerol tetraether lipids in lakes, Proc. Natl. Acad. Sci., 115, 10926–10931, https://doi.org/10.1073/pnas.1805186115, 2018.

Weijers, J. W., Schouten, S., Spaargaren, O. C., and Damsté, J. S. S.: Occurrence and distribution of tetraether membrane lipids in soils: Implications for the use of the TEX86 proxy and the BIT index, Org. Geochem., 37, 1680–1693, https://doi.org/10.1016/j.orggeochem.2006.07.018, 2006.

Weijers, J. W., Panoto, E., van Bleijswijk, J., Schouten, S., Rijpstra, W. I. C., Balk, M., Stams, A. J., and Sinninghe Damsté, J. S.: Constraints on the biological source (s) of the orphan branched tetraether membrane lipids, Geomicrobiol. J., 26, 402–414, https://doi.org/10.1080/01490450902937293, 2009.

Willard, D. A., Bernhardt, C. E., Weimer, L., Cooper, S. R., Gamez, D., and Jensen, J.: Atlas of pollen and spores of the Florida Everglades, Palynology, 28, 175–227, https://doi.org/10.2113/28.1.175, 2004.

Williams, G., Fensome, R., and McRae, R.: The Lentin and Williams Index of Fossil Dinoflagellates, 2017 edn, Am. Assoc. Stratigr. Palynol. Contrib. Ser., 48, 2017.

Wood, G.: Palynological techniques-processing and microscopy. In. Jasonius, J. and McGregor, DC eds., Palynology: Principles and Application., Am. Assoc. Stratigr. Palynol. Found., 1, 29–50, 1996.

Wuchter, C., Abbas, B., Coolen, M. J. L., Herfort, L., van Bleijswijk, J., Timmers, P., Strous, M., Teira, E., Herndl, G. J., Middelburg, J. J., Schouten, S., and Sinninghe Damsté, J. S.: Archaeal nitrification in the ocean, Proc. Natl. Acad. Sci., 103, 12317–12322, https://doi.org/10.1073/pnas.0600756103, 2006.

Xiao, X., Fahl, K., and Stein, R.: Biomarker distributions in surface sediments from the Kara and Laptev seas (Arctic Ocean): indicators for organic-carbon sources and sea-ice coverage, Quat. Sci. Rev., 79, 40–52, https://doi.org/10.1016/j.quascirev.2012.11.028, 2013.

Xie, S., Liu, X.-L., Schubotz, F., Wakeham, S. G., and Hinrichs, K.-U.: Distribution of glycerol ether lipids in the oxygen minimum zone of the Eastern Tropical North Pacific Ocean, Org. Geochem., 71, 60–71, https://doi.org/10.1016/j.orggeochem.2014.04.006, 2014.

Xu, K., Harris, C. K., Hetland, R. D., and Kaihatu, J. M.: Dispersal of Mississippi and Atchafalaya sediment on the Texas–Louisiana shelf: Model estimates for the year 1993, Cont. Shelf Res., 31, 1558–1575, https://doi.org/10.1016/j.csr.2011.05.008, 2011.

Xu, Y., Jia, Z., Xiao, W., Fang, J., Wang, Y., Luo, M., Wenzhöfer, F., Rowden, A. A., and Glud, R. N.: Glycerol dialkyl glycerol tetraethers in surface sediments from three Pacific trenches: Distribution, source and environmental implications, Org. Geochem., 147, 104079, https://doi.org/10.1016/j.orggeochem.2020.104079, 2020.

Yunker, M. B., Macdonald, R. W., Veltkamp, D. J., and Cretney, W. J.: Terrestrial and marine biomarkers in a seasonally ice-covered Arctic estuary—integration of multivariate and biomarker approaches, Mar. Chem., 49, 1–50, https://doi.org/10.1016/0304-4203(94)00057-K, 1995.

Zavala-Hidalgo, J., Romero-Centeno, R., Mateos-Jasso, A., Morey, S. L., and Martínez-López, B.: The response of the Gulf of Mexico to wind and heat flux forcing: What has been learned in recent years?, Atmósfera, 27, 317–334, https://doi.org/10.1016/S0187-6236(14)71119-1, 2014.

Zell, C., Kim, J.-H., Moreira-Turcq, P., Abril, G., Hopmans, E. C., Bonnet, M.-P., Sobrinho, R. L., and Damsté, J. S. S.: Disentangling the origins of branched tetraether lipids and crenarchaeol in the lower Amazon River: Implications for GDGT-based proxies, Limnol. Oceanogr., 58, 343–353, https://doi.org/10.4319/lo.2013.58.1.0343, 2013.

Zell, C., Kim, J.-H., Dorhout, D., Baas, M., and Damsté, J. S. S.: Sources and distributions of branched tetraether lipids and crenarchaeol along the Portuguese continental margin: Implications for the BIT index, Cont. Shelf Res., 96, 34–44, https://doi.org/10.1016/j.csr.2015.01.006, 2015.

Zhu, C., Weijers, J. W., Wagner, T., Pan, J.-M., Chen, J.-F., and Pancost, R. D.: Sources and distributions of tetraether lipids in surface sediments across a large river-dominated continental margin, Org. Geochem., 42, 376–386, https://doi.org/10.1016/j.orggeochem.2011.02.002, 2011.

Zonneveld, K. A. and Pospelova, V.: A determination key for modern dinoflagellate cysts, Palynology, 39, 387–409, https://doi.org/10.1080/01916122.2014.990115, 2015.

Zonneveld, K. A., Chen, L., Möbius, J., and Mahmoud, M. S.: Environmental significance of dinoflagellate cysts from the proximal part of the Po-river discharge plume (off southern Italy, Eastern Mediterranean), J. Sea Res., 62, 189–213, https://doi.org/10.1016/j.seares.2009.02.003, 2009.

Zonneveld, K. A. F., Versteegh, G. J. M., Kasten, S., Eglinton, T. I., Emeis, K.-C., Huguet, C., Koch, B. P., de Lange, G. J., de Leeuw, J. W., Middelburg, J. J., Mollenhauer, G., Prahl, F. G., Rethemeyer, J., and Wakeham, S. G.: Selective

preservation of organic matter in marine environments; processes and impact on the sedimentary record, Biogeosciences, 7, 483–511, https://doi.org/10.5194/bg-7-483-2010, 2010.

Zonneveld, K. A. F., Marret, F., Versteegh, G. J. M., Bogus, K., Bonnet, S., Bouimetarhan, I., Crouch, E., de Vernal, A., Elshanawany, R., Edwards, L., Esper, O., Forke, S., Grøsfjeld, K., Henry, M., Holzwarth, U., Kielt, J.-F., Kim, S.-Y., Ladouceur, S., Ledu, D., Chen, L., Limoges, A., Londeix, L., Lu, S.-H., Mahmoud, M. S., Marino, G., Matsouka, K., Matthiessen, J., Mildenhal, D. C., Mudie, P., Neil, H. L., Pospelova, V., Qi, Y., Radi, T., Richerol, T., Rochon, A., Sangiorgi, F., Solignac, S., Turon, J.-L., Verleye, T., Wang, Y., Wang, Z., and Young, M.: Atlas of modern dinoflagellate cyst distribution based on 2405 data points, Rev. Palaeobot. Palynol., 191, 1–197, https://doi.org/10.1016/j.revpalbo.2012.08.003, 2013.